

Equation-of-motion internally contracted multireference unitary coupled-cluster theory

Shuhang Li,^{1, a)} Zijun Zhao,¹ and Francesco A. Evangelista^{1, b)}

Department of Chemistry and Cherry Emerson Center for Scientific Computation, Emory University, Atlanta, Georgia 30322, United States

The accurate computation of excited states remains a challenge in electronic structure theory, especially for systems with a ground state that requires a multireference treatment. In this work, we introduce a novel equation-of-motion (EOM) extension of the internally contracted multireference unitary coupled-cluster framework (ic-MRUCC), termed EOM-ic-MRUCC. EOM-ic-MRUCC follows the transform-then-diagonalize approach, in analogy to its non-unitary counterpart [Datta and Nooijen, *J. Chem. Phys.* **137**, 204107 (2012)]. By employing a projective approach to optimize the ground state, the method retains additive separability and proper scaling with system size. We show that excitation energies are size intensive if the EOM operator satisfies the “killer” and the projective conditions. Furthermore, we propose to represent changes in reference state upon electron excitation via projected many-body operators that span active orbitals and show that the EOM equations formulated in this way are invariant with respect to active orbital rotations. We test the EOM-ic-MRUCC method truncated to single and double excitations by computing the potential energy curves for several excited states of a BeH₂ model system, the HF molecule, and water undergoing symmetric dissociation. Across these systems, our method delivers accurate excitation energies and potential energy curves within 5 mE_h (ca. 0.14 eV) from full configuration interaction. We find that truncating the Baker–Campbell–Hausdorff series to four-fold commutators contributes negligible errors (on the order of 10⁻⁵ E_h or less), offering a practical route to highly accurate excited-state calculations with reduced computational overhead.

I. INTRODUCTION

The accurate description of the electronic structure of molecules in excited states remains a long-standing challenge in quantum chemistry, primarily due to the intricate interplay of static and dynamical electron correlation effects. Most well-established excited-state methods fall under the single-reference (SR) category and assume that the ground state is dominated by a single configuration, often a closed-shell Hartree–Fock determinant. Owing to their computational efficiency and simplicity, configuration interaction with single excitations (CIS)¹ and time-dependent density functional theory (TD-DFT)^{2,3} are among the most popular SR approaches. Excited-state methods based on coupled-cluster (CC) theory⁴⁻⁶ include CC linear response (CC-LR)⁷⁻¹⁰ and equation-of-motion CC theory (EOM-CC),¹¹⁻¹⁶ which are equivalent as far as excitation energies are concerned.¹⁷ A closely related formalism, the symmetry-adapted cluster configuration interaction (SAC-CI), was also proposed by Nakatsuji.¹⁸ Furthermore, CC methods that directly target individual states have been proposed.¹⁹⁻²⁹ Excited-state CC methods are the preferred choice for high-accuracy computations due to their conceptual simplicity and ability to accurately capture excitations while retaining size-extensivity and size-intensivity properties.³⁰ However, their performance can deteriorate significantly when multiple determinants are required to describe the ground state, *e.g.*, at transition state geometries, bond-

recoupling regions, and open-shell transition metal complexes.

Multireference CC (MRCC) methods³¹⁻³⁶ that start from a correlated reference wavefunction provide the basis for extending EOM-CC to the multireference domain. Jagau *et al.*^{37,38} reported a linear response formalism based on Mukherjee’s MRCC theory (Mk-MRCC-LR). Because this approach is based on the Jeziorski–Monkhorst ansatz,³⁹ the number of amplitudes scales linearly with the number of reference determinants, leading to exponential scaling with the number of active orbitals. At the same time, Mk-MRCC-LR excited-state energies also depend on the choice of active orbitals since the ground-state energy is not invariant with respect to active-active orbital rotations. Internally contracted MRCC (ic-MRCC) and related formalisms⁴⁰⁻⁵² address these issues by expressing the ground state as a single exponential operator acting on a linear combination of reference determinants. Excited-state methods based on variants of internally contracted formalisms include the MR-EOMCC approach developed by Nooijen and co-workers⁵³ and linear response ic-MRCC (ic-MRCC-LR) introduced by Samanta *et al.*⁵⁴ The reliance of excited-state MRCC methods on non-Hermitian effective Hamiltonians is problematic as it can potentially result in unphysical complex eigenvalues.^{53,55}

The goal of this paper is to examine excited-state methods based on *unitary* MRCC (MRUCC). Unitary formulations of CC theory (UCC)⁵⁶⁻⁶² offer notable advantages over traditional CC, such as faster convergence towards full configuration interaction (FCI) and preservation of Hermiticity.⁶³⁻⁶⁷ Excited-state formulations of UCC⁶⁸⁻⁷⁰ lead to a consistent calculation of proper-

^{a)}Electronic mail: shuhang.li@emory.edu

^{b)}Electronic mail: francesco.evangelista@emory.edu

ties via either the sum-over-states polarization propagator and response theory,⁷¹ and approximate variants of UCC have been shown to be connected to the GW method.⁶⁷ UCC was originally introduced in the early days of quantum chemistry but remained mostly an academic curiosity since it leads to a non-terminating Baker–Campbell–Hausdorff (BCH) expansion of the similarity-transformed Hamiltonian.⁷² In this direction, a related work is the multireference algebraic diagrammatic construction (MR-ADC) theory developed by Sokolov and co-workers for the simulation of various spectroscopic processes.^{17,73–77} MR-ADC is a Hermitian multireference propagator method, in which the ground state is formally equivalent to ic-MRUCC. Practical MR-ADC truncation schemes treat both ground and excited states at the perturbative level, with the highest level treatment achieved to date being the extended second order.⁷³

Recently, renewed interest in UCC has stemmed from the observation by Peruzzo *et al.*⁷⁸ that UCC realized as a product of unitary operators can be implemented on a quantum computer in polynomial time using a series of gate-based operations. Various quantum computing approaches have been proposed to approximate both ground and excited state molecular energies based on UCC,^{79–93} many of which are quantum variants of classical EOM or LR approaches. Several of these methods may be considered forms of EOM multireference UCC. For example, qEOM⁹⁰ solves a set of EOM equations where the ground state is approximated with a UCC state with singles and doubles (UCCSD). The q-sc-EOM^{91,94} and quantum linear response (qLR) formalisms⁹⁵ adopted the self-consistent EOM operator formulation,^{96,97} and proposed a projective operator variant. In both cases, a factorized UCC ground state was built adaptively starting from a Hartree–Fock reference.⁹⁸ While the abovementioned papers considered all orbitals in the system, a series of recent works investigated qLR with excitation expansion truncated to an active space in combination with orbital response in the full orbital space.^{92,93,99–102} This may be viewed as an MCSCF linear response formalism in which the reference is an orbital-optimized UCCSD state spanning only the active orbitals.^{103,104}

In this work, we present an EOM extension of the ic-MRUCC approach based on a correlated reference generated within the conventional active-space partitioning of the orbitals. We adopt a projective approach to determine the ground-state ic-MRUCC amplitudes,¹⁰⁵ which, unlike variational formulations,¹⁰⁶ is both size consistent and size extensive. Previous quantum computing implementations of EOM-UCC use a product form of the UCC state to capture electron correlation from either all orbitals or only the active orbitals. In contrast, our approach explicitly separates the contributions from the active orbitals, treating the remaining correlation effects in the ground and excited states with operators that promote the electrons to and from at least one orbital outside the active space. These operators are responsible for both

orbital relaxation and two-body correlation effects. This development is also designed to inform EOM extensions of approximate UCC-based theories. We are specifically interested in the multireference driven similarity renormalization group (MR-DSRG) formalism,^{107–111} an approximate, renormalized variant of ic-MRUCC robust to numerical instabilities.

The remainder of the paper is organized as follows. Section II details the projective formulation of ic-MRUCC theory and the strategies used to eliminate operator linear dependencies. This section also presents the EOM extension of ic-MRUCC, discusses the conditions required to achieve size-intensive excitation energies, and describes our parameterization of the EOM excitation operator. Section III provides details of our EOM-ic-MRUCC pilot implementation. In Section IV, we report benchmark results comparing EOM-ic-MRUCC calculations to FCI results for three model systems and examine how truncating the BCH expansion affects accuracy. Finally, in Section V, we summarize our findings and highlight future research directions, including potential extensions to approximate UCC-based theories within the DSRG framework.

II. THEORY

A. Notation

To establish our formalism, we begin by introducing the notation and conventions employed throughout this work. We consider a multideterminantal reference state, $|\Phi_0\rangle$, obtained from a complete-active-space self-consistent-field (CASSCF) computation. This state is a linear combination of Slater determinants $|\phi_\mu\rangle$ weighted by normalized coefficients c_μ :

$$|\Phi_0\rangle = \sum_{\mu=1}^d |\phi_\mu\rangle c_\mu. \quad (1)$$

The set of determinants $M = \{|\phi_\mu\rangle, \mu = 1, \dots, d\}$ defines the model space, and it is constructed from a set of spin orbitals partitioned into core (**C**), active (**A**), and virtual (**V**) subsets of sizes $N_{\mathbf{C}}$, $N_{\mathbf{A}}$, and $N_{\mathbf{V}}$, respectively. The notation CAS(me, no) denotes a complete active space with m electrons distributed among n spatial active orbitals. We use the indices m, n to designate core spin orbitals, u, v, w, x, y, z, t to represent active spin orbitals, and e, f, g, h for virtual spin orbitals. We also introduce two composite orbital subsets: the hole spin orbitals ($\mathbf{H} = \mathbf{C} \cup \mathbf{A}$) and the particle spin orbitals ($\mathbf{P} = \mathbf{A} \cup \mathbf{V}$) of dimensions $N_{\mathbf{H}} = N_{\mathbf{C}} + N_{\mathbf{A}}$ and $N_{\mathbf{P}} = N_{\mathbf{A}} + N_{\mathbf{V}}$, respectively. The hole spin orbitals are denoted by the labels i, j, k, l , while the particle spin orbitals are labeled with a, b, c, d . General spin orbitals that belong to either the hole or particle set are designated as p, q, r, s .

B. Internally contracted multireference unitary coupled-cluster theory

The ic-MRUCC ansatz parameterizes the exact many-body ground state with a unitary exponential operator, $e^{\hat{A}}$, acting on the general reference state $|\Phi_0\rangle$:

$$|\Psi_0\rangle = e^{\hat{A}} |\Phi_0\rangle = e^{\hat{T} - \hat{T}^\dagger} |\Phi_0\rangle. \quad (2)$$

The operator $\hat{A} = \hat{T} - \hat{T}^\dagger$ is the anti-Hermitian combination of the cluster operator \hat{T} . The operator \hat{T} may include hole-particle excitation operators with up to n -fold substitutions, where n is the number of electrons in the system.

To express the ic-MRUCC equations in a compact form, we introduce general amplitudes ($t_q \equiv t_{ab\dots}^{ij\dots}$) and excitation operators ($\hat{\tau}_q \equiv \{\hat{a}_{ij\dots}^{ab\dots}\}$) identified by a collective index $q = (ij\dots, ab\dots)$ that ranges from one to the total number of excitation operators (n_{ex}):

$$\hat{T} = \sum_{q=1}^{n_{\text{ex}}} t_q \hat{\tau}_q. \quad (3)$$

Brackets ($\{\cdot\}$) are used to indicate normal ordering with respect to the correlated state Φ_0 , using the generalized normal-ordering (GNO) formalism.^{112–114} The cluster amplitudes $t_{ab\dots}^{ij\dots}$ in the ic-MRUCC ansatz are tensors antisymmetric with respect to the individual permutation of upper and lower indices. Internal amplitudes corresponding to substitutions involving only active orbitals are not included, *i.e.*, $t_{uv\dots}^{xy\dots} = 0$,³³ as their role is to relax the coefficients of the reference determinants, which is made redundant by the reference relaxation procedure discussed below.⁴³

Inserting the ic-MRUCC ansatz [see Eq. (2)] into the Schrödinger equation and left-multiplying by $e^{-\hat{A}}$ leads to

$$e^{-\hat{A}} \hat{H} e^{\hat{A}} |\Phi_0\rangle = \bar{H} |\Phi_0\rangle = E_0 |\Phi_0\rangle, \quad (4)$$

where we have introduced the transformed Hamiltonian $\bar{H} = e^{-\hat{A}} \hat{H} e^{\hat{A}}$. Cluster amplitude equations are obtained by left-projecting Eq. (4) onto a linearly independent set of internally contracted excited functions. An obvious choice is the set of internally contracted excited configurations $\{\hat{\tau}_q |\Phi_0\rangle\}$; however, these states are not guaranteed to be linearly independent since the corresponding metric matrix

$$(\mathbf{S})_{pq} = \langle \Phi_0 | \hat{\tau}_p^\dagger \hat{\tau}_q | \Phi_0 \rangle, \quad (5)$$

is generally singular. This linear dependency introduces numerical instabilities, prompting the need to eliminate redundant configurations in most internally contracted MR methods.^{43–45,115–117}

Following earlier implementations of ic-MRCC,^{43–45} we address the issue of linear dependencies by expressing \hat{T}

in terms of linearly independent operators $\hat{\kappa}_Q$ and corresponding amplitudes k_Q as:

$$\hat{T} = \sum_{Q=1}^{n_{\text{in}}} k_Q \hat{\kappa}_Q, \quad (6)$$

where n_{in} is the number of linearly independent operators. Writing the linearly independent excitation operators as a row vector, $\hat{\boldsymbol{\kappa}} = (\hat{\kappa}_1, \dots, \hat{\kappa}_{n_{\text{in}}})$, we can express them in terms of the original excitation operators $[\hat{\boldsymbol{\tau}} = (\hat{\tau}_1, \dots, \hat{\tau}_{n_{\text{ex}}})]$ via the rectangular matrix \mathbf{X} as:

$$\hat{\boldsymbol{\kappa}} = \hat{\boldsymbol{\tau}} \mathbf{X}. \quad (7)$$

Various methods exist for defining \mathbf{X} , and prior studies have determined ways to ensure the size extensivity of the corresponding ic-MRCC theory.⁴⁵ These strategies can also be extended to formulate a size-extensive ic-MRUCC theory, as discussed in Appendix A. What is important to note is that since we define ic-MRUCC using normal-ordered operators, size extensivity is guaranteed irrespective of the orthogonalization procedure used to obtain \mathbf{X} .

Projecting Eq. (4) onto the set of linearly independent internally contracted states leads to the following set of amplitude equations:

$$\langle \Phi_0 | \hat{\kappa}_Q^\dagger \bar{H} | \Phi_0 \rangle = 0. \quad (8)$$

The energy and expansion coefficients are instead obtained by projecting Eq. (4) onto the model space determinants, resulting in the following eigenvalue equation

$$\sum_{\nu} \langle \phi_{\mu} | \bar{H} | \phi_{\nu} \rangle c_{\nu} = E_0 c_{\mu}. \quad (9)$$

To relax the reference state in the presence of dynamical correlation effects included via the exponential operator, Eqs. (8) and (9) must be solved iteratively until self-consistency is reached. This is also a necessary condition for the ic-MRUCC state to be exact.

In concluding this section, we discuss the exactness of the ic-MRUCC ansatz in relation to ic-MRCC and single-reference UCC theory. In the case of ic-MRCC, the convergence of the wavefunction toward the full configuration interaction limit as the maximum excitation rank increases was proved by constructing the corresponding exact cluster operator \hat{T} .¹¹⁸ Extending such proof to the case of a unitary operator runs into difficulties already encountered in the case of single-reference UCC, where numerical evidence has been unable to find counterexamples to exactness, but a formal proof of exactness is unknown.¹¹⁹ Therefore, at present, the exactness of the ic-MRUCC ansatz can only be assumed as a working hypothesis and tested numerically.

C. Equation-of-motion extension of ic-MRUCC

Following EOM theory,^{11–16} we define the EOM-ic-MRUCC ansatz as

$$|\Psi_\alpha\rangle = \bar{\mathcal{R}}_\alpha |\Psi_0\rangle, \quad (10)$$

where $\bar{\mathcal{R}}_\alpha$ is a formal excitation operator delivering the α -th excited state from the ic-MRUCC ground state, *i.e.*, formally $\bar{\mathcal{R}}_\alpha \equiv |\Psi_\alpha\rangle\langle\Psi_0|$. The Schrödinger equation for this excited state reads

$$\hat{H}\bar{\mathcal{R}}_\alpha |\Psi_0\rangle = E_\alpha \bar{\mathcal{R}}_\alpha |\Psi_0\rangle, \quad (11)$$

whereas the ground-state Schrödinger equation, left-multiplied by $\bar{\mathcal{R}}_\alpha$, reads

$$\bar{\mathcal{R}}_\alpha \hat{H} |\Psi_0\rangle = E_0 \bar{\mathcal{R}}_\alpha |\Psi_0\rangle, \quad (12)$$

where E_0 and E_α are the ground- and excited-state energies, respectively. Taking the difference of these two equations eliminates the ground-state energy and yields:

$$[\hat{H}, \bar{\mathcal{R}}_\alpha] |\Psi_0\rangle = \omega_\alpha \bar{\mathcal{R}}_\alpha |\Psi_0\rangle, \quad (13)$$

where $\omega_\alpha = E_\alpha - E_0$ denotes the excitation energy of the α -th state.

Due to its formal advantages, we adopt the “self-consistent” excitation operators introduced by Mukherjee and coworkers,^{96,97} which expresses $\bar{\mathcal{R}}_\alpha$ as a similarity-transformed operator:

$$\bar{\mathcal{R}}_\alpha \equiv e^{\hat{A}} \hat{\mathcal{R}}_\alpha e^{-\hat{A}}. \quad (14)$$

Substituting this expression into Eq. (13) and multiplying on the left by $\exp(-\hat{A})$ we arrive at:

$$[\bar{H}, \hat{\mathcal{R}}_\alpha] |\Phi_0\rangle = \omega_\alpha \hat{\mathcal{R}}_\alpha |\Phi_0\rangle. \quad (15)$$

The advantage of the self-consistent operator approach is that it yields an expression for the excitation energy [Eq. (15)] in terms of the similarity-transformed Hamiltonian $\bar{H} = e^{-\hat{A}} \hat{H} e^{\hat{A}}$.

Next, we consider the problem of how we should parameterize the operator $\bar{\mathcal{R}}_\alpha$ to make the EOM approach exact. The excited state generated by $\bar{\mathcal{R}}_\alpha$ may be expressed as:

$$|\Psi_\alpha\rangle = \bar{\mathcal{R}}_\alpha |\Psi_0\rangle = e^{\hat{A}} \hat{\mathcal{R}}_\alpha |\Phi_0\rangle, \quad (16)$$

or equivalently

$$\hat{\mathcal{R}}_\alpha |\Phi_0\rangle = e^{-\hat{A}} |\Psi_\alpha\rangle. \quad (17)$$

We may interpret Eq. (17) as a constraint on the form of $\hat{\mathcal{R}}_\alpha$: this operator must transform the reference $|\Phi_0\rangle$ into a general vector in Hilbert space. Additionally, orthogonality between the ground and excited states implies that $\hat{\mathcal{R}}_\alpha |\Phi_0\rangle$ must be orthogonal to $|\Phi_0\rangle$ since

$\langle\Phi_0|\hat{\mathcal{R}}_\alpha|\Phi_0\rangle = \langle\Phi_0|e^{-\hat{A}}|\Psi_\alpha\rangle = \langle\Psi_0|\Psi_\alpha\rangle = 0$. For convenience, we will refer to the condition:

$$\langle\Phi_0|\hat{\mathcal{R}}_\alpha|\Phi_0\rangle = 0, \quad (18)$$

as the weak form of the killer condition. This condition is implied by the stronger killer condition (also known as the vacuum annihilation condition),^{96,97,120–122} which is often invoked in the formulation of EOM methods:

$$\hat{\mathcal{R}}_\alpha^\dagger |\Phi_0\rangle = 0. \quad (19)$$

When parameterized as a linear operator, $\hat{\mathcal{R}}_\alpha$ must be a combination of excitation operators $\{\hat{\rho}_p\}$ with corresponding excitation amplitudes r_α^p :

$$\hat{\mathcal{R}}_\alpha = \sum_{p=1}^{n_{\text{eom}}} r_\alpha^p \hat{\rho}_p. \quad (20)$$

Projecting Eq. (15) on the left onto the set of internally contracted configurations $\{\hat{\rho}_p|\Phi_0\rangle\}$ and using Eq. (20) lead to the following generalized eigenvalue problem:

$$\sum_{q=1}^{n_{\text{eom}}} \langle\Phi_0|\hat{\rho}_p^\dagger[\bar{H}, \hat{\rho}_q]|\Phi_0\rangle r_\alpha^q = \omega_\alpha \sum_{q=1}^{n_{\text{eom}}} \langle\Phi_0|\hat{\rho}_p^\dagger \hat{\rho}_q|\Phi_0\rangle r_\alpha^q. \quad (21)$$

Orthogonality among the excited states may be expressed as a condition on the inner product of EOM operators:

$$\langle\Psi_\alpha|\Psi_\beta\rangle = \langle\Phi_0|\hat{\mathcal{R}}_\alpha^\dagger \hat{\mathcal{R}}_\beta|\Phi_0\rangle = \sum_{p,q=1}^{n_{\text{eom}}} r_\alpha^p \langle\Phi_0|\hat{\rho}_p^\dagger \hat{\rho}_q|\Phi_0\rangle r_\beta^q = \delta_{\alpha\beta}. \quad (22)$$

If $\hat{\mathcal{R}}_\alpha$ satisfies the killer condition [Eq. (19)], it is possible to rewrite the EOM equation only in terms of commutators as:

$$\sum_{q=1}^{n_{\text{eom}}} \langle\Phi_0|[\hat{\rho}_p^\dagger, [\bar{H}, \hat{\rho}_q]]|\Phi_0\rangle r_\alpha^q = \omega_\alpha \sum_{q=1}^{n_{\text{eom}}} \langle\Phi_0|[\hat{\rho}_p^\dagger, \hat{\rho}_q]|\Phi_0\rangle r_\alpha^q. \quad (23)$$

This second form of the EOM equations is generally preferred to Eq. (21) as it leads to an expansion in terms of fully connected diagrams, ensuring size-intensive excitation energies. Moreover, for a fully relaxed ic-MRUCC state, the matrix entering the left-hand side is Hermitian due to the killer and the projective amplitude conditions. For unrelaxed ic-MRUCC states, one may formulate a Hermitian eigenvalue problem by symmetrizing the double commutator.

To arrive at a practical EOM-ic-MRUCC scheme, we need to specify a form for the excitation operator $\hat{\mathcal{R}}_\alpha$. This operator may be separated into internal ($\hat{\mathcal{R}}_\alpha^{\text{int}}$) and external ($\hat{\mathcal{R}}_\alpha^{\text{ext}}$) components:

$$\hat{\mathcal{R}}_\alpha = \hat{\mathcal{R}}_\alpha^{\text{int}} + \hat{\mathcal{R}}_\alpha^{\text{ext}}, \quad (24)$$

where internal excitations map the model space into itself ($\hat{\mathcal{R}}_\alpha^{\text{int}} M \in M$), while external excitations generate

excited configurations outside the model space ($\hat{\mathcal{R}}_\alpha^{\text{ext}} M \notin M$). Operators from these two groups span orthogonal spaces when applied to the state $|\Phi_0\rangle$. Note that scalar terms should be excluded from $\hat{\mathcal{R}}_\alpha$ to ensure that the weaker form of the killer condition, $\langle\Phi_0|\hat{\mathcal{R}}_\alpha|\Phi_0\rangle = 0$, is satisfied.

We parameterize external excitations with the same set of many-body operators in \hat{T} . For the ic-MRUCCSD method considered in this study, this set comprises all one and two hole-particle substitution operators, excluding those labeled only by active indices. Omitting the target excited state label (α) we can write the external excitations as:

$$\hat{\mathcal{R}}^{\text{ext}} = \hat{\mathcal{R}}_1^{\text{ext}} + \hat{\mathcal{R}}_2^{\text{ext}}, \quad (25)$$

where a generic k -body term is defined as

$$\hat{\mathcal{R}}_k^{\text{ext}} = \frac{1}{(k!)^2} \sum_{ij\dots}^{\mathbf{H}} \sum_{ab\dots}^{\mathbf{P}} r_{ij\dots}^{ij\dots} \{\hat{a}_{ij\dots}^{ab\dots}\}. \quad (26)$$

When parameterized this way, the adjoint of $\hat{\mathcal{R}}^{\text{ext}}$ contains operators of the form $\{\hat{a}_{ab\dots}^{ij\dots}\}$, which annihilate the reference state. Therefore, $\hat{\mathcal{R}}^{\text{ext}}$ naturally satisfies the killer condition.

There are several possible parameterizations for internal excitations, leading to different ways to realize EOM-ic-MRUCC. A common and convenient choice is to represent internal EOM excitations using transfer operators between the ground and excited CASCI solutions:^{17,73,123,124}

$$\hat{\mathcal{R}}_{\text{CAS}}^{\text{int}} = \sum_{I>0} r_I |\Phi_I\rangle \langle\Phi_0|. \quad (27)$$

This parameterization satisfies the killer condition, but it is impractical for large active spaces due to the combinatorial growth of the number of excited CASCI solutions with the number of electrons and active orbitals.^{17,73} Since the convergence of the excitation energies with the number of transfer operators is generally fast, a practical solution is to work with a small set of CASCI states representing low-lying excited states. This comes at the cost of compromising orbital invariance in the EOM step, as the truncated CASCI states no longer constitute a complete basis for the model space.

In this work, we propose to use an alternative solution based on projected many-body (pMB) internal excitations. This approach is analogous to the projected operator set first proposed by Szekeres *et al.*,¹²² and then by several recent works on quantum EOM and LR theories.^{92,93,95,99,125,126} To satisfy the killer condition, we start from many-body internal operators ($\{\hat{a}_{uv\dots}^{xy\dots}\}$) defined to contain only active indices. From the internal operators, we define the corresponding projected form as $\hat{\rho}_q = \{\hat{a}_{uv\dots}^{xy\dots}\} |\Phi_0\rangle \langle\Phi_0| - \langle\Phi_0|\{\hat{a}_{uv\dots}^{xy\dots}\}|\Phi_0\rangle$. Since the operators $\{\hat{a}_{uv\dots}^{xy\dots}\}$ are normal ordered w.r.t. $|\Phi_0\rangle$, the second term vanishes by

definition,¹¹² *i.e.*, $\hat{\rho}_q = \{\hat{a}_{uv\dots}^{xy\dots}\} |\Phi_0\rangle \langle\Phi_0|$. Moreover, these new operators satisfy the killer conditions since $\hat{\rho}_q^\dagger |\Phi_0\rangle = |\Phi_0\rangle \langle\Phi_0|\{\hat{a}_{xy\dots}^{uv\dots}\}|\Phi_0\rangle = 0$, where in the last term $\langle\Phi_0|\{\hat{a}_{xy\dots}^{uv\dots}\}|\Phi_0\rangle = 0$ due to the normal-ordering condition. In the case of singles and doubles, the projected many-body internals are defined as:

$$\hat{\mathcal{R}}_{\text{pMBS}}^{\text{int}} = \sum_{ux}^{\mathbf{A}} r_x^u \{\hat{a}_u^x\} |\Phi_0\rangle \langle\Phi_0|, \quad (28)$$

and

$$\hat{\mathcal{R}}_{\text{pMBD}}^{\text{int}} = \frac{1}{4} \sum_{uvxy}^{\mathbf{A}} r_{xy}^{uv} \{\hat{a}_{uv}^{xy}\} |\Phi_0\rangle \langle\Phi_0|. \quad (29)$$

The main advantage of the pMB formulation is that it reduces the number of variables from combinatorial to polynomial scaling. Higher order pMB operators can be included in $\hat{\mathcal{R}}^{\text{int}}$ to improve the description of excitations involving active orbitals systematically. When the space of internal excitations is saturated, the pMB approach becomes equivalent to the transfer operator approach. In principle, it is also possible to determine eigenstates of \hat{H} within the space spanned by the pMB states ($\{\hat{a}_{uv\dots}^{xy\dots}\} |\Phi_0\rangle$) and then truncate them by keeping a small number of low-energy eigenstates, as done in the transfer operator approach. This approach is not explored in this work.

The matrix representation of the connected EOM-ic-MRUCC equation [Eq. (23)] is:

$$\bar{\mathbf{H}}' \mathbf{r}_\alpha = \omega_\alpha \mathbf{S}' \mathbf{r}_\alpha, \quad (30)$$

where the matrices $\bar{\mathbf{H}}'$ and \mathbf{S}' are defined as

$$\bar{H}'_{pq} = \langle\Phi_0|[\hat{\rho}_p^\dagger, [\bar{H}, \hat{\rho}_q]]|\Phi_0\rangle, \quad (31)$$

and

$$S'_{pq} = \langle\Phi_0|[\hat{\rho}_p^\dagger, \hat{\rho}_q]|\Phi_0\rangle. \quad (32)$$

Note that the $\bar{\mathbf{H}}'$ and \mathbf{S}' matrices are constructed using the $\hat{\rho}_p$ operators (either internal or external excitations) and can in principle differ from the matrices $\bar{\mathbf{H}}$ and \mathbf{S} that appear in ic-MRUCC. Like for the ground-state problem, the set of internally contracted excited configurations $\{\hat{\rho}_p |\Phi_0\rangle\}$ exhibit linear dependence and can be orthogonalized via a linear transformation induced by the matrix \mathbf{M} :

$$\hat{\chi} = \hat{\rho} \mathbf{M}. \quad (33)$$

When expressed in the $\hat{\chi}$ operator basis, Eq. (30) becomes an ordinary eigenvalue problem:

$$\bar{\mathbf{H}}'' \mathbf{r}'_\alpha = \omega_\alpha \mathbf{r}'_\alpha, \quad (34)$$

where the modified matrix $\bar{\mathbf{H}}''$ and vector \mathbf{r}'_α are defined as $\bar{\mathbf{H}}'' = \mathbf{M}^\dagger \bar{\mathbf{H}}' \mathbf{M}$ and $\mathbf{r}'_\alpha = \mathbf{M}^\dagger \mathbf{r}_\alpha$.

D. Size intensivity of excitation energies and orbital invariance of EOM-ic-MRUCC

In this section, we discuss the scaling properties of the EOM-ic-MRUCC excitation energies. The additive separability of the ground-state energy is instead discussed in Appendix A, where we also report numerical tests to confirm that a GNO-based formulation of this approach leads to size-consistent energies.

For the EOM extension of ic-MRUCC, we require that excitation energies remain constant in the presence of non-interacting subsystems (size intensivity) and that they remain unchanged by unitary rotations that separately mix core, active, and virtual orbitals (orbital invariance). The requirement of size intensivity has implications on the choice of the excitation operator manifold. As we prove in Appendix B, the killer condition is necessary for satisfying size intensivity. As discussed in Section II C, our parameterization of the $\hat{\mathcal{R}}_\alpha$ operator automatically satisfies Eq. (19). Each operator in the orthogonalized EOM manifold, $\{\hat{\chi}_Q\}$, further needs to satisfy the following condition:

$$\langle \Phi_0 | \hat{\chi}_Q^\dagger \bar{H} | \Phi_0 \rangle = 0. \quad (35)$$

To show that $\hat{\mathcal{R}}_\alpha$ also satisfies Eq. (35), we rewrite the l.h.s. by inserting the resolution of the identity in terms of CASCI eigenstates (Φ_I) and linearly independent EOM external excited configurations ($\hat{\chi}_Q | \Phi_0 \rangle$):

$$\begin{aligned} \langle \Phi_0 | \hat{\chi}_P^\dagger \bar{H} | \Phi_0 \rangle &= \sum_I^{\text{CAS}} \langle \Phi_0 | \hat{\chi}_P^\dagger | \Phi_I \rangle \langle \Phi_I | \bar{H} | \Phi_0 \rangle \\ &+ \sum_Q^{\text{ext}} \langle \Phi_0 | \hat{\chi}_P^\dagger \hat{\chi}_Q | \Phi_0 \rangle \langle \Phi_0 | \hat{\chi}_Q^\dagger \bar{H} | \Phi_0 \rangle. \end{aligned} \quad (36)$$

If the ground state reference is an eigenstate of \bar{H} , i.e., it satisfies Eq. (9), then the first term of Eq. (36) reduces to $\langle \Phi_0 | \hat{\chi}_P^\dagger | \Phi_0 \rangle \langle \Phi_0 | \bar{H} | \Phi_0 \rangle$, and the factor $\langle \Phi_0 | \hat{\chi}_P^\dagger | \Phi_0 \rangle$ is null since $\hat{\chi}_P^\dagger$ is a linear combination of GNO operators. The second term in Eq. (36) is zero because the factor $\langle \Phi_0 | \hat{\chi}_Q^\dagger \bar{H} | \Phi_0 \rangle$ is guaranteed to be null by the amplitude equation [Eq. (8)] and the equivalence of the external excitation orthonormalized operator basis of \hat{T} and $\hat{\mathcal{R}}_\alpha^{\text{ext}}$.

To emphasize the importance of GNO in the definition of the internal EOM excitations, we conducted a numerical test to assess size intensivity, employing the eigenoperator basis ($\hat{\mathcal{R}}_{\text{CAS}}^{\text{int}}$) and the projected many-body singles ($\hat{\mathcal{R}}_{\text{pMBS}}^{\text{int}}$) with and without using normal-ordered operators. For this test, we use the LiH + H₂ composite system and expand the active spaces for LiH and the composite system to CAS(2,4) and CAS(4,6), respectively (see Appendix A). The differences in the first triplet excitation energy between the composite system and the LiH subsystem were found to be $1.3 \times 10^{-7} E_h$ when employing $\hat{\mathcal{R}}_{\text{pMBS}}^{\text{int}}$ without normal-ordered operators. This difference was instead less than $10^{-12} E_h$ when employing

either the $\hat{\mathcal{R}}_{\text{CAS}}^{\text{int}}$ or $\hat{\mathcal{R}}_{\text{pMBS}}^{\text{int}}$ with GNO operators, consistent with our formal analysis. The GNO transformation is therefore employed for all EOM-ic-MRUCC computations without explicit labeling.

Lastly, we note another advantage of formulating the EOM-ic-MRUCC using projected many-body excitations. For large active spaces that might require truncation, using pMB operators preserves the orbital invariance property if all elements of a certain excitation type are included, in contrast to a truncated eigenoperator basis that will not satisfy this condition.

III. IMPLEMENTATION

The EOM-ic-MRUCC method has been implemented in a pilot code interfaced with FORTE,¹²⁷ an open-source plugin for the PSI4 *ab initio* quantum chemistry package.¹²⁸ Our implementation leverages FORTE's functionality to represent arbitrary linear combinations of determinants and second-quantized operators using a bit array representation. A general state $|\Omega\rangle$ is expressed as a linear combination of determinants ($|\phi_\mu\rangle$) as:

$$|\Omega\rangle = \sum_\mu c_\mu |\phi_\mu\rangle. \quad (37)$$

The action of $e^{\hat{A}}$ on a state vector $|\Omega\rangle$ is computed using the Taylor expansion:

$$e^{\hat{A}} |\Omega\rangle = |\Omega\rangle + \hat{A} |\Omega\rangle + \frac{1}{2!} \hat{A}^2 |\Omega\rangle + \dots, \quad (38)$$

and is truncated when the largest absolute element of the vector $\frac{1}{m!} \hat{A}^m |\Omega\rangle$ is less than 10^{-9} . To evaluate the BCH series up to given truncated order we use the following identity⁶⁴ to express a single term with k nested commutators:

$$\underbrace{[[\dots [[\hat{H}, \hat{A}], \hat{A}], \dots], \hat{A}]}_{k \text{ nested commutators}} = \sum_{l=0}^k (-1)^l \binom{k}{l} \hat{A}^l \hat{H} \hat{A}^{k-l}. \quad (39)$$

Our implementation of the ic-MRUCC method closely follows the algorithm used in the ic-MRUCC method.⁴³ To solve the ic-MRUCC amplitude equations, an approximated quasi-Newton method is employed. Following Ref. 45, instead of working with GNO operators directly, we use a simpler strategy based on the transformation matrix \mathbf{G} which connects the normal-ordered operators ($\hat{\mathbf{O}}_{\text{GNO}}$) to the corresponding bare operators ($\hat{\mathbf{O}}$):

$$\hat{\mathbf{O}}_{\text{GNO}} = \hat{\mathbf{O}} \mathbf{G}. \quad (40)$$

After solving the ic-MRUCC amplitude equations, the \mathbf{G} matrix is constructed to transform all excitation operators for the EOM extension of ic-MRUCC to the GNO basis. The detailed derivation of the GNO transformation matrix \mathbf{G} and its explicit block structure are provided in Appendix C.

IV. RESULTS

A. The BeH₂ model

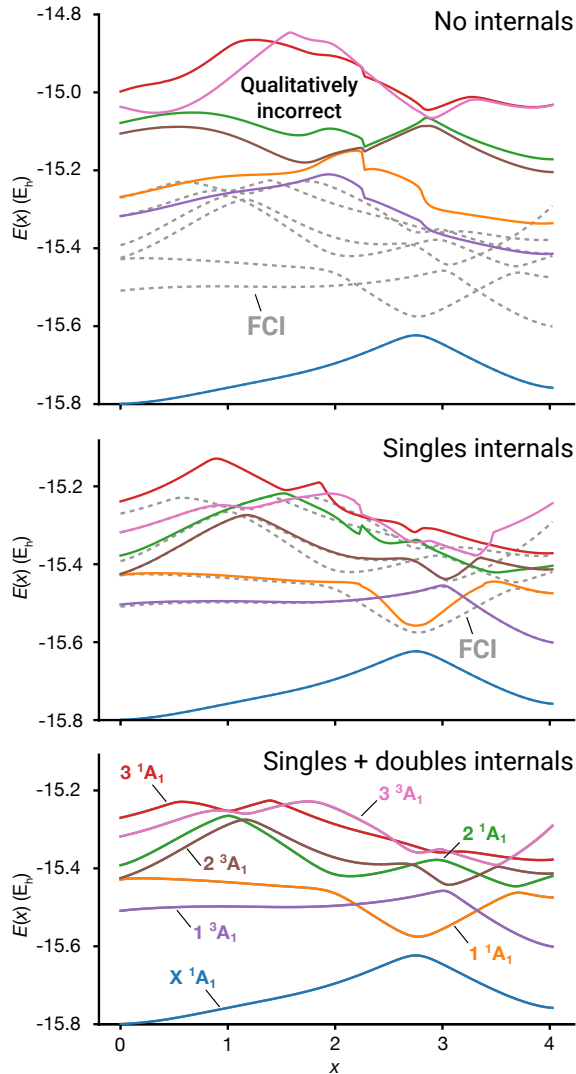


FIG. 1. Potential energy curves of seven low-lying states of the BeH₂ model computed with the EOM-ic-MRUCCSD using different definitions of the EOM internal excitation operator. FCI energies are indicated with dashed gray lines.

For our first test of the EOM-ic-MRUCCSD method we consider the BeH₂ model system,^{129,130} a well-established benchmark for new multireference methods.^{43,106,131–137} The BeH₂ model captures the salient features of the perpendicular insertion of a beryllium atom into a H₂ molecule by a one-dimensional path constrained to C_{2v} symmetry. For this model, we compute the potential energy curves (PECs) for the ground (X ¹A₁) and six excited states of singlet and triplet symmetry (1 ¹A₁, 2 ¹A₁, 3 ¹A₁, 1 ³A₁, 2 ³A₁, and 3 ³A₁). A zeroth-order description of the ground state of this system requires two closed-shell determinants. However, in our compu-

tations, to capture both the ground and excited states, we employ a full-valence complete active space reference state that includes the 1s orbitals of H and the 2s and 2p orbitals of Be [CASSCF(4e,6o)], and all electrons are correlated. In the BeH₂ model, the beryllium atom is placed at the center of a two-dimensional Cartesian coordinate system, and the coordinates of the two hydrogen atoms are described by the curve $y(x) = \pm(2.54 - 0.46x)$, where $x \in [0, 4]$ a_0 is the reaction coordinate. A custom double-zeta quality basis set, Be(10s3p/3s2p), H(4s/2s), is used here, following earlier works.^{43,106} A linear dependence threshold $\eta = 10^{-4}$ is used in the ic-MRUCC computations.

We begin by investigating how the choice of internal EOM excitations affects the accuracy of the excited states. In Fig. 1, we plot the PECs for the seven electronic states of the BeH₂ model system using EOM-ic-MRUCCSD with three different choices of internal EOM excitations. When internal excitations are omitted entirely ($\hat{\mathcal{R}}^{\text{int}} = 0$), all excited states are shifted to significantly higher energy, and the corresponding curves incorrectly predict many of the qualitative features of the FCI results. The inclusion of single internal excitations ($\hat{\mathcal{R}}_{\text{pMBS}}^{\text{int}}$) introduces the necessary degrees of freedom to capture the qualitative features of several low-energy excited states (1 ¹A₁, 1 ³A₁, and 2 ³A₁). However, this modification still results in qualitatively inaccurate curves for the higher-energy states (2 ¹A₁, 3 ¹A₁, and 3 ³A₁). Finally, in the bottom panel of Fig. 1, we see that adding the internal doubles ($\hat{\mathcal{R}}_{\text{pMBD}}^{\text{int}}$) provides qualitatively correct PECs indistinguishable from the FCI ones.

To understand how internal excitations improve the description of excited states, we analyze the leading determinants in the EOM-ic-MRUCCSD wavefunction. In Fig. 2, we plot the leading determinants for two representative excited states (1 ¹A₁ and 1 ³A₁) of the BeH₂ model system (at $x = 2.250 a_0$) using the three different choices of EOM internal excitations. The EOM-ic-MRUCCSD calculations start from the same X ¹A₁ reference state (Φ_0), where the two leading determinants are as follows:

$$|\Phi_0\rangle = 0.9672 |(1a_1)^2(2a_1)^2(1b_2)^2\rangle - 0.1206 |(1a_1)^2(2a_1)^2(3a_1)^2\rangle + \dots, \quad (41)$$

which differs slightly from the FCI ground state (with coefficients for the two leading determinants being 0.9652 and -0.1204). The FCI results in Fig. 2 show that both the 1 ¹A₁ and 1 ³A₁ states are connected to the ground state via internal excitations. Consequently, omitting internal excitations entirely excludes important determinants and leads to the qualitatively incorrect curves shown in Fig. 1. The inclusion of internal single excitations ($\hat{\mathcal{R}}_{\text{pMBS}}^{\text{int}}$) successfully generates the correct leading determinants for the 1 ³A₁ state but leads to an incorrect zeroth-order description for the 1 ¹A₁ state, which is dominated by doubly excited determinants with respect to the leading reference determinant $|(1a_1)^2(2a_1)^2(1b_2)^2\rangle$. Finally, adding the internal double

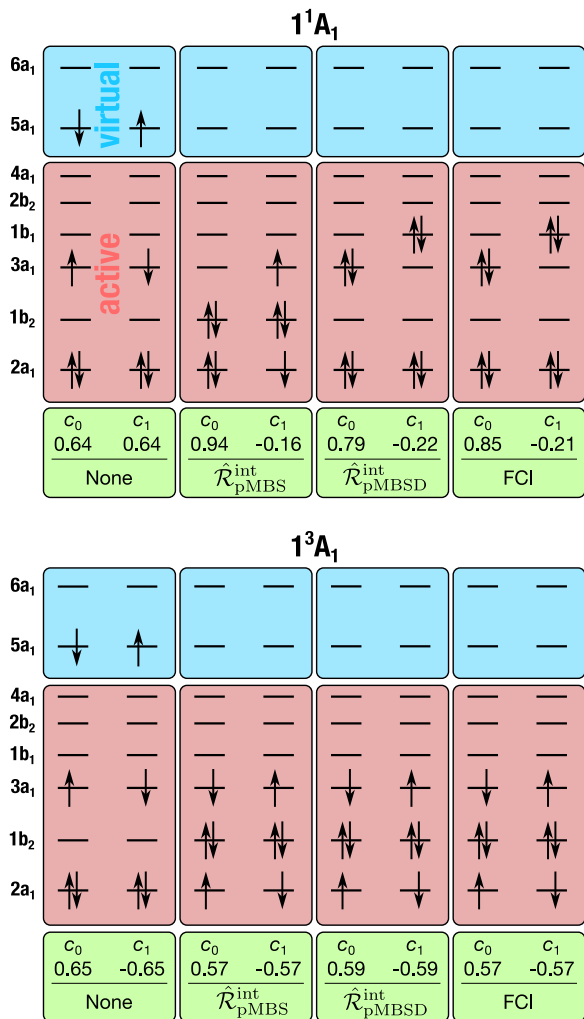


FIG. 2. Leading determinants for the 1^1A_1 and 1^3A_1 excited states of the BeH_2 model system (at $x = 2.25 a_0$) using three different choices of internal EOM excitations and the FCI. Orbitals in the red section represent active orbitals, while orbitals in the blue section represent virtual orbitals. The core orbital ($1a_1$) and virtual orbitals higher than $6a_1$ are not included in the figure.

excitations ($\hat{\mathcal{R}}_{\text{pMBS}}^{\text{int}}$) results in the correct leading determinants for the 1^1A_1 state, explaining the superior accuracy of the PECs computed at this level.

It is important to note that all energy curves from EOM-ic-MRUCCSD are discontinuous. This is a common challenge encountered in multireference theories, including the MR-EOMCC method⁵³ and ic-MRCC approaches.⁴³ This problem is due to the change in the number of linearly independent operators that enter the \hat{T} and $\hat{\mathcal{R}}$ operators across the potential energy surface.⁴³ In the case of BeH_2 , this effect is more pronounced in the truncation schemes that omit internal excitations or include only internal singles, particularly around $x = 2.250 a_0$. In the PECs computed with up to internal doubles, the discontinuities are less pronounced. To analyze the

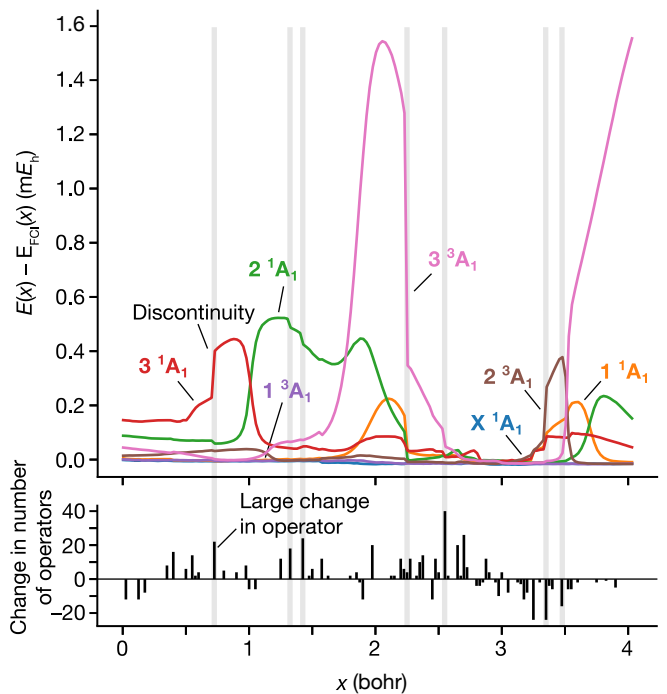


FIG. 3. Top panel: potential energy error curves (with respect to FCI) of seven low-lying states of the BeH_2 model computed with the EOM-ic-MRUCCSD method and internal singles and doubles. Lower panel: the change in the number of orthogonal operators that enter $\hat{\mathcal{R}}$ with respect to the previous point (to the left).

origin of these discontinuities, in Fig. 3 we plot the change in energy error and number of orthogonal operators for the 2^1A_1 and 3^1A_1 states. This plot shows that discontinuities are correlated with changes in the number of linearly independent operators in $\hat{\mathcal{R}}$.

In Fig. 4, we compare the accuracy of EOM-ic-MRUCCSD with state-of-the-art excited-state methods, including EOM-CCSD, EOM-CC3, SA-DSRG-PT2, and SA-DSRG-PT3, by plotting energy differences from the FCI value for the X^1A_1 and 1^1A_1 states of the BeH_2 system. To quantify the accuracy of these methods, each curve in Fig. 4 is accompanied by the corresponding non-parallelity error (NPE), defined over a range of geometries (X) as:

$$\text{NPE} = \max_{x \in X} [\Delta E(x)] - \min_{x \in X} [\Delta E(x)], \quad (42)$$

where $\Delta E(x)$ is the error with respect to the FCI energy. Note that for EOM-CCSD and EOM-CC3, we use the following Slater determinant as the zeroth-order wavefunction:

$$|\Phi_1\rangle = |(1a_1)^2(2a_1)^2(1b_2)^2\rangle. \quad (43)$$

However, this is the dominant determinant for the ground state only for those geometries with $x < 2 a_0$. Consequently, the BeH_2 model system is particularly challenging for these single-reference methods. Notably, both

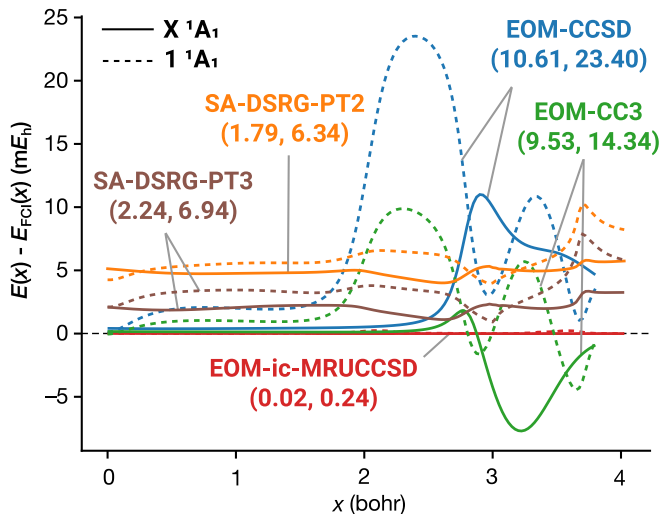


FIG. 4. Potential energy error curves of different methods with respect to FCI for $X\ ^1A_1$ and $1\ ^1A_1$ states of the BeH_2 model system. For each method the nonparallelity errors (in mE_h) are shown in parentheses ($X\ ^1A_1$, $1\ ^1A_1$).

$X\ ^1A_1$ and $1\ ^1A_1$ PECs for EOM-CCSD and EOM-CC3 exhibit significant errors within the strongly correlated region ($x > 2.825\ a_0$),⁴³ yield large NPEs, and fail when $x > 3.800\ a_0$ due to a lack of convergence of the ground state computations. The SA-DSRG-PT2/3 methods directly target ground- and excited-state solutions by employing a state-averaged description of dynamical electron correlation. These methods display errors consistent across the potential energy curve, including the multireference region, and yield NPEs smaller than the single-reference methods. In comparison, the EOM-ic-MRUCCSD method stands out as the most accurate, yielding the smallest NPEs (0.02 and 0.24 mE_h for $X\ ^1A_1$ and $1\ ^1A_1$ states, respectively) among all methods.

B. The dissociation curve of HF

Our second benchmark considers the ground ($X\ ^1A_1$) and excited ($1\ ^1A_1$, $1\ ^3A_1$, and $2\ ^3A_1$) PECs of hydrogen fluoride.^{43,138} A consistent zeroth-order description of the ground state of this system requires considering the σ H-F bonding and antibonding orbitals. However, similar to the BeH_2 model system, we employ a larger active space that includes the 1s orbital of H and the 2s, 2p, and 3s orbitals of F [CASSCF(8e,6o)]. In all computations, the fluorine 1s-like molecular orbital is excluded from the correlated computations, and the linear dependence threshold η is set to 10^{-4} . We employ the DZV basis set adopted in Ref. 138.

As shown in Fig. S1 of the Supplementary Information, EOM-ic-MRUCCSD yields qualitatively correct PECs for the HF molecule. Deviations of the EOM-ic-MRUCCSD PECs from FCI are small for the ground

state ($< 1.4\ mE_h$), while they are larger for the excited states, with maximum errors of 4.6, 2.1, and 3.8 mE_h for the $1\ ^1A_1$, $1\ ^3A_1$, and $2\ ^3A_1$ states, respectively (in all cases less than 0.15 eV). Similar to the BeH_2 system, all PECs are discontinuous. In Fig. 5, we plot the potential energy error curves for four states and track how the number of orthogonal operators entering \hat{R} changes. These discontinuities align with shifts in the number of linearly independent operators, consistent with our findings for the BeH_2 model.

We also compared the EOM-ic-MRUCCSD method with two SA-DSRG methods. The potential energy error curves for different states obtained with SA-DSRG-PT2, SA-DSRG-PT3, and EOM-ic-MRUCCSD, are shown in Fig. 6. EOM-CCSD and EOM-CC3 computations did not yield continuous PECs at stretched geometries and, therefore, are not included in this figure. The EOM-ic-MRUCCSD curves exhibit minimal errors and have the lowest NPE values (0.61, 3.07, 0.94, and 3.22 mE_h for $X\ ^1A_1$, $1\ ^1A_1$, $1\ ^3A_1$, and $2\ ^3A_1$ states, respectively) among all methods.

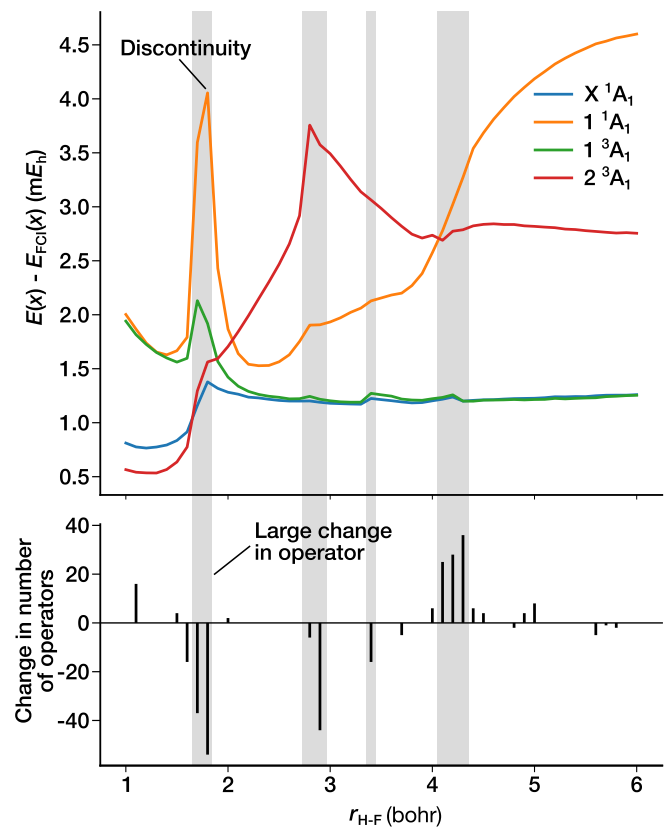


FIG. 5. Top panel: potential energy error curves (with respect to FCI) of four low-lying states of the HF system computed with the EOM-ic-MRUCCSD method and internal singles and doubles. Lower panel: the change in the number of orthogonal operators that enter \hat{R} with respect to the previous point (to the left).

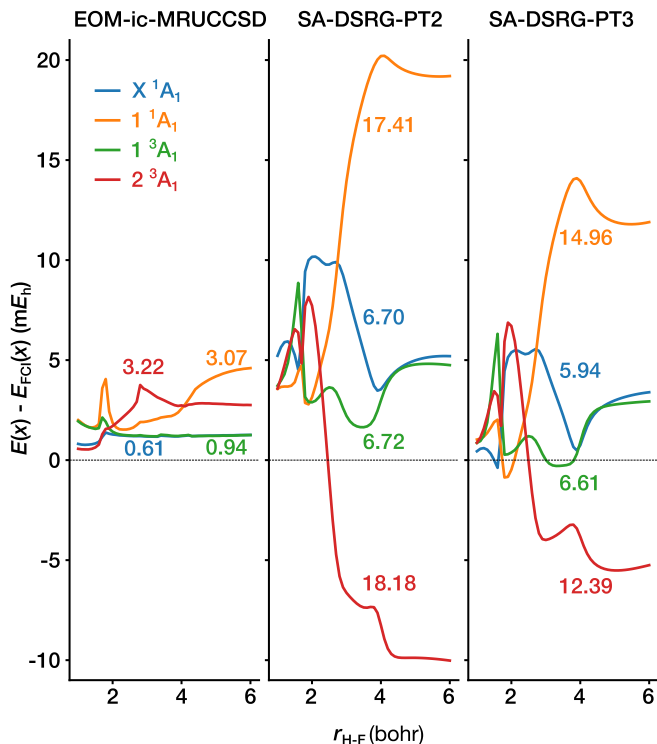


FIG. 6. Potential energy error curves of different methods with respect to FCI for X ¹A₁, 1 ¹A₁, 1 ³A₁, and 2 ³A₁ states of the HF molecule. For each method, the nonparallelity errors (in mE_h) are shown alongside the curves.

C. Symmetric dissociation of the water molecule

Our next application focuses on the symmetric dissociation of the water molecule. This system has been utilized as a benchmark for various theories and serves as a prototype for multiple bond-breaking processes.^{43,47,134,139–143} Following Ref. 43, we calculate PECs for the two lowest singlet states (X ¹A₁ and 1 ¹A₁) and two lowest triplet excited states (1 ³A₁ and 2 ³A₁) for the symmetric dissociation path with the H–O–H bond angle constrained to 109.57°, while scanning the O–H bond distance within the range of [r_e , $4r_e$] at $0.1 r_e$ spacing, where $r_e = 0.9929 \text{ \AA}$. We employ the 6-31G basis and select an active space that includes the 1s orbital of hydrogen and the 2p manifold for the oxygen atom, resulting in a CASSCF(6e,5o) reference wavefunction. The oxygen 1s-like molecular orbital is excluded from correlated computations. The linear dependence threshold η is set to 10^{-5} for the ground (X ¹A₁) and two triplet excited states (1 ³A₁ and 2 ³A₁). For the singlet excited state, we employ two thresholds (η_1 and η_2). The η_1 threshold (10^{-5}) is used to eliminate linear dependencies in the singles, semi-internal doubles (with at least one active orbital creation and annihilator), and internal excitations. The remaining doubles typically exhibit less severe linear dependencies, and we employ a smaller truncation threshold η_2 (10^{-8}). Employing two different

thresholds is essential for obtaining a qualitatively correct PEC for the 1 ¹A₁ excited state. We will examine this aspect after analyzing the results obtained with two thresholds.

In Fig. 7, we plot the potential energy error curves for all states along with the change in the number of orthogonal operators that enter into $\hat{\mathcal{R}}$. Throughout the sampled range of geometries, the EOM-ic-MRUCCSD PECs for the X ¹A₁, 1 ³A₁, and 2 ³A₁ states show very small deviations from FCI (less than $1.4 mE_h$, within chemical accuracy). In contrast, the 1 ¹A₁ state shows errors as large as ca. $3 mE_h$. Consistent with our previous findings, all PECs exhibit small discontinuities that correlate with changes in the number of linearly independent EOM operators.

We also compared the EOM-ic-MRUCCSD method with the SA-DSRG-PT2 and SA-DSRG-PT3 methods, while we excluded EOM-CCSD and EOM-CC3 since they cannot be consistently converged along the dissociation path. As shown in Fig. 8, the EOM-ic-MRUCCSD curves yield the smallest NPEs (0.32, 2.77, 1.15, and 0.73 mE_h for the X ¹A₁, 1 ¹A₁, 1 ³A₁, and 2 ³A₁ states, respectively) among all methods. The PECs obtained from SA-DSRG-PT3 generally have smaller NPEs compared to SA-DSRG-PT2, except for the 2 ³A₁ state (6.75 and 10.17 mE_h for SA-DSRG-PT2 and PT3, respectively). However, errors from SA-DSRG methods consistently exceed those from EOM-ic-MRUCCSD.

Next, we discuss the challenges encountered in the computations on the 1 ¹A₁ state. As shown in Fig. S2 of the Supplementary Information, EOM-ic-MRUCCSD produces a qualitatively incorrect PEC when using a single orthogonalization threshold in the EOM step ($\eta = 10^{-5}$). A notable discontinuity appears in the dissociation region around $r(\text{O–H}) = 3.5 r_e$ for the single-threshold calculation, while this discontinuity is absent in the double-threshold calculation. As shown in Fig. S3 of the Supplementary Information, the pronounced discontinuity in the single-threshold calculation is correlated with the change in the number of linearly dependent operators that enter into $\hat{\mathcal{R}}$. The energy error significantly increases at $r(\text{O–H}) = 3.5 r_e$ as 46 operators are removed from the EOM operator space, resulting in a notable discontinuity in the PEC.

To understand the impact of these removed operators on the excited-state energy in the single-threshold calculation, we reintroduce them into the operator space and measure the resulting energy corrections for the 1 ¹A₁ state. We find that operators contributing significant energy corrections (larger than $0.1 mE_h$) are linear combinations of the form $\hat{a}_{u_\alpha u_\beta}^{e_\alpha f_\beta}$ where u is one of the active orbitals ($1b_2, 2b_2, 3a_1, 4a_1$), and e and f are virtual orbitals. These operators replace an electron pair from a single active orbital with two virtual spin orbitals. The reason why in the dissociated region, these operators are excluded from the EOM ansatz of the PEC is that the X ¹A₁ ic-MRUCCSD state becomes largely dominated by open-shell determinants with singly occupied $1b_2, 2b_2,$

$3a_1$, and $4a_1$ orbitals. For example, at $r(\text{O-H}) = 3.5 r_e$, the ground state is given by

$$|\Psi_0\rangle = 0.5464 [(2a_1)^2(1b_1)^2 1b_{2\alpha} 3a_{1\beta} 2b_{2\beta} 4a_{1\alpha}] + [(2a_1)^2(1b_1)^2 1b_{2\beta} 3a_{1\alpha} 2b_{2\alpha} 4a_{1\beta}] + \dots \quad (44)$$

Determinants with paired active electrons contribute only minorly to $|\Psi_0\rangle$, and so applying $\hat{a}_{u_\alpha u_\beta}^{e_\alpha f_\beta}$ to this state generates a term with near zero norm. Consequently, these operators are removed during the orthogonalization step, causing a cumulative error on the order of $5 mE_h$. This issue arises because the operators are orthogonalized using a metric derived solely from the ground-state wavefunction; as a result, they can be discarded simply because they (approximately) annihilate the ground state, even though they are important for describing certain excited states. We note that while this problem may be solved using two sets of thresholds, yielding a qualitatively correct PEC in the range $r(\text{O-H}) \in [r_e, 4r_e]$, this discontinuity is expected to reappear at a larger bond distance, where the eigenvalues of pair excitation operators approach zero. Indeed, at $r(\text{O-H}) = 6 r_e$, and even setting $\eta_2 = 10^{-10}$ fails to capture all important pair excitation operators, resulting in a similar $6 mE_h$ energy error in the double-threshold PEC. It is important to note that since this issue is independent of the specific treatment of correlation (the orthogonalization is based on the reference state only), it is expected to affect *all* EOM-like multireference methods based on internally contracted ansätze.

D. Truncation of the commutator series

Since the BCH expansion of the unitarily transformed Hamiltonian does not terminate, any practical implementation of EOM-ic-MRUCC must evaluate this operator in an approximate way. One approach is to approximate \bar{H} with a BCH expansion truncated at a given order. To evaluate the impact of this approximation, we perform a statistical analysis of the error introduced in the ground- and excited-state PECs of the BeH_2 , HF, and water systems.

The BCH expansion is truncated to the same order in all expressions involving \bar{H} , including the ic-MRUCC energy and amplitude equations and the EOM-ic-MRUCC eigenvalue equation. Table I shows the root-mean-square error (RMSE) for the energy of all states computed with a truncated \bar{H} with respect to the non-truncated EOM-ic-MRUCCSD results. The inclusion of the second commutator yields satisfactory results for the BeH_2 system, with all RMSEs approximately $10^{-5} E_h$. However, this level of truncation is inaccurate for HF and water, as the RMSEs become larger than $1.0 mE_h$. The RMSE is exceptionally large for the excited states of water, with values of 0.415, 0.486, and $0.436 E_h$ for 1^1A_1 , 1^3A_1 , and 2^3A_1 states, respectively.

The introduction of the triple commutator does not

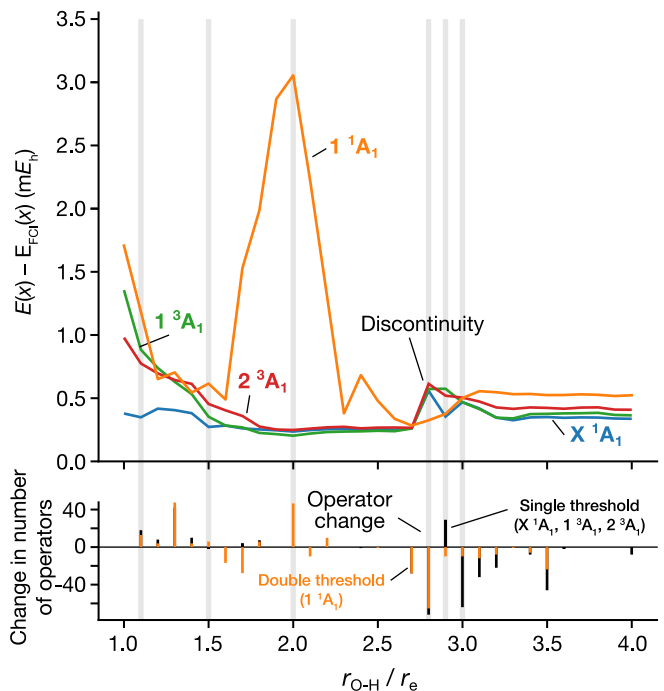


FIG. 7. Top panel: potential energy error curves (with respect to FCI) for the X^1A_1 , 1^1A_1 , 1^3A_1 , and 2^3A_1 states of water along the symmetric dissociation path computed with the EOM-ic-MRUCCSD method and internal computed many-body singles and doubles. Two thresholds $\eta_1 = 10^{-5}$ and $\eta_2 = 10^{-8}$ are used in the EOM step to eliminate linear dependencies for the 1^1A_1 state, while all other curves used a single orthogonalization threshold $\eta = 10^{-5}$. Lower panel: the change in the number of orthogonal operators and the energy errors with respect to the previous point (to the left).

significantly enhance results for the BeH_2 and HF systems but substantially improves the accuracy of the water system PECs. In this case, all RMSEs for the water system are reduced to around $10^{-4} E_h$. Notably, the inclusion of the four-nested commutator leads to a significant reduction in all RMSEs, bringing them to around $10^{-6} E_h$ for the BeH_2 model and $10^{-5} E_h$ for the HF and water systems. These results are promising and indicate that EOM-ic-MRUCC schemes with a truncated BCH expansion may serve as robust and reliable approximations to the full EOM-ic-MRUCC. The truncation of the BCH expansion preserves the scaling and orbital invariance properties of EOM-ic-MRUCC.

V. CONCLUSION

We have reported a new orbital invariant and size-intensive equation-of-motion extension of the internally contracted multireference unitary coupled-cluster (EOM-ic-MRUCC) method. In this approach, the underlying ground state is computed at the ic-MRUCC level, using a projective approach based on generalized normal-ordered operators, which, unlike previous formulations,¹⁰⁶ is rig-

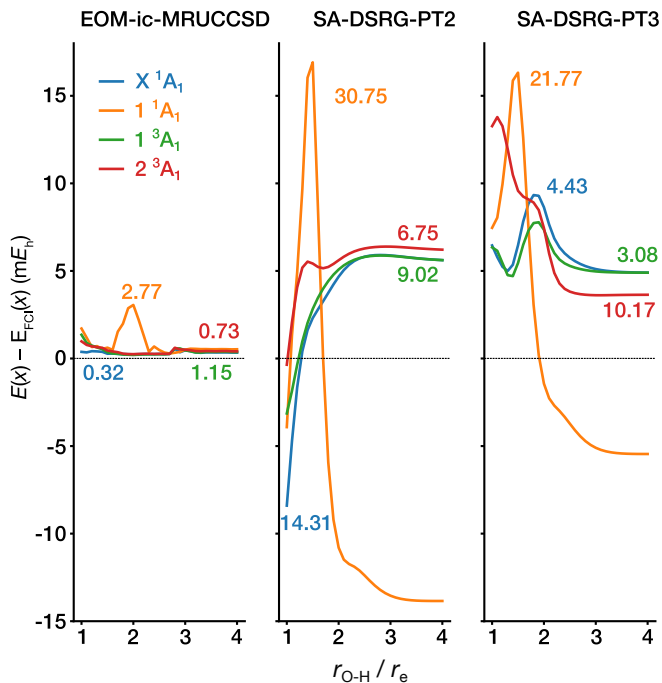


FIG. 8. Potential energy error curves of different methods with respect to FCI for X^1A_1 , 1^1A_1 , 1^3A_1 , and 2^3A_1 states of the symmetric dissociation of the water. For each method, the nonparallelity errors (in mE_h) are shown alongside the curves.

ously size consistent and size extensive. The EOM-ic-MRUCC method follows the transform-then-diagonalize route, like its non-unitary counterpart (MR-EOMCC).⁵³ In formulating the EOM extension of ic-MRUCC, we adopt the self-consistent operator approach and analyze different operator choices. We propose using projected many-body operators to represent the internal components of the excitation operator that modify the occupation of active orbitals. This choice ensures polynomial scaling in the number of active orbitals while preserving orbital invariance. Moreover, since projected many-body operators satisfy the killer condition, the excitation energies are size intensive.

Benchmark results for the Be + H₂ insertion reaction, the dissociation of HF, and the symmetric dissociation of water are obtained using a pilot code implementation of EOM-ic-MRUCC theory based on the expansion of the corresponding equations in the full configuration-interaction basis. Within our benchmark results, EOM-ic-MRUCC truncated to single and double excitations (EOM-ic-MRUCCSD) yields highly accurate potential energy curves that deviate from FCI by less than 5 mE_h and have nonparallelity errors less than 4 mE_h . When applied to compute excited states over an entire potential energy curve, EOM-ic-MRUCC outperforms both single-reference methods (EOM-CCSD, EOM-CC3) and low-order perturbative approximations (SA-DSRG-PT2 and SA-DSRG-PT3) across all examined excited states. We find that truncating the BCH expansion to low commu-

TABLE I. Statistical analysis of the error introduced in the EOM-ic-MRUCCSD results ground- and excited-state energies when truncating the BCH expansion of the unitarily-transformed Hamiltonian. Root-mean-square error (RMSE, in E_h) computed for the potential energy curves of BeH₂, HF, and H₂O. The RMSE is computed separately for each electronic state using N equally spaced samples of the poten-

tial energy curve as $\text{RMSE} = \sqrt{N^{-1} \sum_{i=1}^N (\delta E_i^{(k)})^2}$, where $\delta E_i^{(k)}$ is the energy error with respect to the non-truncated theory for the i -th point on the curve when \bar{H} is evaluated with up to k nested commutators.

BeH ₂				
States	2	3	4	
X^1A_1	4.567×10^{-5}	1.944×10^{-5}	7.819×10^{-6}	
1^1A_1	1.286×10^{-5}	2.235×10^{-5}	8.631×10^{-6}	
2^1A_1	1.328×10^{-5}	2.120×10^{-5}	9.213×10^{-6}	
3^1A_1	1.455×10^{-5}	2.014×10^{-5}	9.713×10^{-6}	
1^3A_1	1.860×10^{-5}	1.862×10^{-5}	7.102×10^{-6}	
2^3A_1	1.804×10^{-5}	1.684×10^{-5}	7.142×10^{-6}	
3^3A_1	1.882×10^{-5}	1.643×10^{-5}	7.937×10^{-6}	
HF				
States	2	3	4	
X^1A_1	2.928×10^{-4}	1.840×10^{-4}	1.633×10^{-5}	
1^1A_1	5.121×10^{-3}	2.234×10^{-3}	9.514×10^{-5}	
1^3A_1	8.798×10^{-4}	2.712×10^{-4}	1.608×10^{-5}	
2^3A_1	2.677×10^{-3}	1.437×10^{-3}	3.640×10^{-5}	
H ₂ O				
States	2	3	4	
X^1A_1	3.957×10^{-4}	2.518×10^{-4}	1.895×10^{-5}	
1^1A_1	4.153×10^{-1}	2.309×10^{-4}	2.330×10^{-5}	
1^3A_1	4.859×10^{-1}	1.958×10^{-4}	1.316×10^{-5}	
2^3A_1	4.363×10^{-1}	1.884×10^{-4}	1.711×10^{-5}	

tator orders introduces negligible errors: inclusion of up to four commutators yields RMSEs less than 0.01 mE_h for the three systems considered in this work. Properties such as orbital invariance, size consistency, and size extensivity are preserved when the BCH expansion is truncated.

Despite its many desirable properties, we identify two major challenges with the EOM-ic-MRUCC method. Firstly, in truncated schemes, the use of projected many-body operators introduces high-order RDMs. Although it may be tempting to approximate higher-order RDMs with lower-order RDMs by neglecting higher-order cumulants,¹⁴⁴ such approximations do not satisfy N -representability and can lead to variational collapse.¹⁴⁵ Secondly, potential energy curves obtained from EOM-ic-MRUCC are discontinuous due to abrupt changes in the number of orthogonal operators, potentially leading to qualitatively incorrect results. Discontinuities are observed in both ground and excited state potential energy curves. Unfortunately, these discontinuities are expected to affect any theory that expresses excited states via excitation operators applied to an internally contracted state.

These discontinuities may result in a qualitatively incorrect potential energy surface, and can be mitigated by introducing separate orthogonalization thresholds for different classes of excitations. Future work will focus on addressing these issues by reformulating the EOM-ic-MRUCC method using the driven similarity renormalization group framework.

ACKNOWLEDGMENTS

We thank Dr. Alexander Yu. Sokolov for valuable discussions on the discontinuity issue of EOM-ic-MRUCC theory. This research was supported by the U.S. Department of Energy under Award DE-SC0024532. S.L. thanks the National Science Foundation and the Molecular Sciences Software Institute for the financial support under Grant No. CHE-2136142.

DATA AVAILABILITY

All data are available upon reasonable request. The software used to produce the data presented in this work is available in an accompanying public code repository.¹⁴⁶

APPENDIX A: Scaling Properties and Choice of Orthogonalization Scheme

This appendix discusses the formal scaling properties of ic-MRUCC and its EOM extension,^{147–150} focusing on the role played by the choice of the orthonormal excitation operators and the pool of operators used to define the EOM extension. A key requirement for the size extensivity of the energy (correct asymptotic scaling of correlation energy with system size) is that the diagrammatic expansion of the energy contains only connected diagrams. When the energy of a size-extensive method is invariant with respect to orbital rotations among sets of orbitals that preserve the structure of the reference state, size extensivity also implies additivity of the energy for separable states of non-interacting fragments (size consistency).

Previous studies have shown that the size extensivity of ic-MRCC depends on the choice of the operators that enter in \hat{T} and the \mathbf{X} matrix defined in Eq. (7) of the main text.^{43,44} In particular, Hanauer and Köhn⁴⁵ demonstrated that for a basis of generalized normal-ordered operators, either a full or sequential orthogonalization procedure ensures size extensivity. Similar considerations apply to the unitary version of ic-MRCC, and in our work, we ensure size extensivity by employing the GNO orthogonalization scheme described in Appendix C. The proof of the size extensivity for the GNO-based ic-MRCC follows along the same lines as for ic-MRCC,⁴⁵ differing only in the transformed Hamiltonian \bar{H} expression. Like in ic-MRCC theory, the transformed Hamiltonian is

also connected in the unitary version due to the nested commutator structure of the Baker–Campbell–Hausdorff (BCH) formula:

$$\bar{H} = e^{-\hat{A}} \hat{H} e^{\hat{A}} = \hat{H} + \sum_{k=1}^{\infty} \frac{1}{k!} \underbrace{[[\dots [[\hat{H}, \hat{A}], \hat{A}], \dots], \hat{A}]}_{k \text{ nested commutators}}. \quad (\text{A1})$$

Note that when formulated via the variational method,¹⁰⁶ ic-MRUCC theory is expected to lack size extensivity due to the appearance of disconnected terms upon taking the derivative of the truncated effective Hamiltonian with respect to the amplitudes.

To test size consistency numerically, we have implemented all three orthogonalization schemes considered in the literature, here denoted as “full”,⁴³ “sequential”,^{44,151} and “GNO”.⁴⁵ The “full” and “sequential” schemes apply Löwdin canonical orthogonalization to the non-normal-ordered operator basis in one step or sequentially (first singles, then doubles), respectively. The “GNO” scheme applies Löwdin canonical orthogonalization to GNO normal-ordered operators. For each scheme, we have conducted three sets of numerical tests for core, valence, and full size consistency of the energy. The systems used to test these properties are shown in Fig. 9. 1) The core-consistency test partitions the systems such that one H_2 molecule is assigned core and virtual orbitals only, while the second H_2 molecule is assigned only active and virtual orbitals. 2) The valence-consistency test considers one H_2 molecule with valence and virtual orbitals and one LiH molecule treated as a general system (with core, active, and virtual orbitals). 3) The full size-consistency test employs two LiH molecules, both partitioned as a general system.

Table II reports the difference in energy between the composite system and the sum of its fragments. We find that only the GNO-based scheme passes all three size-consistency tests, while the full and sequential approaches fail at least one test.

TABLE II. Core- and valence-consistency errors (in E_h) in ic-MRUCCSD with different orthogonalization procedures. A bold entry indicates that a test has passed.

Orthogonalization Procedure	Size-consistency test		
	Core	Valence	Full
Full	5.7×10^{-8}	2.4×10^{-7}	1.7×10^{-4}
Sequential	< 10^{-12}	1.5×10^{-8}	2.1×10^{-6}
GNO	< 10^{-12}	< 10^{-12}	3.2×10^{-11}

APPENDIX B: Proof of size intensity for choices of the internal excitation operators

In this appendix, we prove that excitation energies computed with EOM-ic-MRUCC are size intensive. We consider two non-interacting systems A and B, with the overall wavefunction multiplicatively separable, *i.e.*,

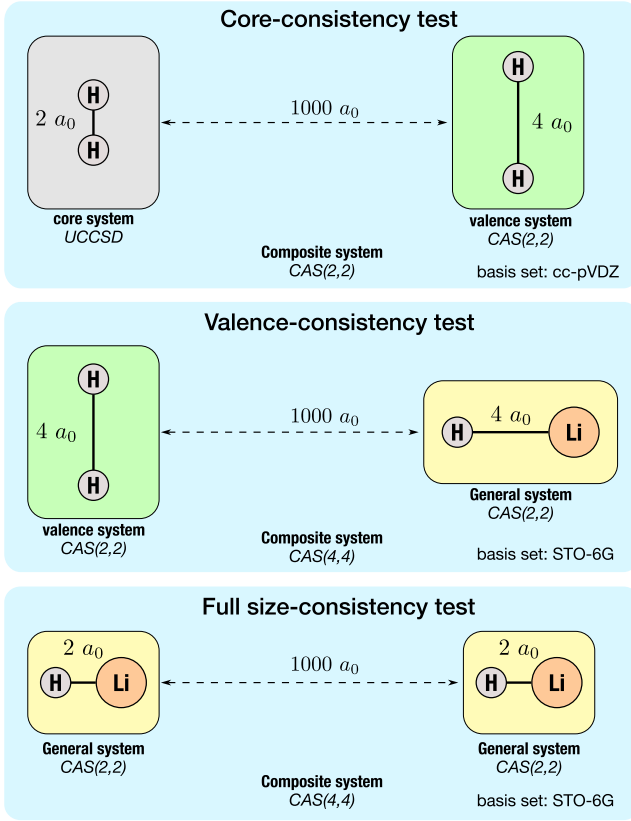


FIG. 9. Systems used in testing the size-consistency properties of ic-MRUCC. A total of nine ic-MRUCCSD computations (italic labels) were performed. A “core” system has only core and virtual orbitals (no active orbitals), a “valence” system has all electrons in the active space (no core orbitals), and a “general” system has core, active, and virtual orbitals.

$\Psi_{AB} = \Psi_A \Psi_B$. The cumulants involving orbitals localized on either A or B are identically null for such a state. As a result, the effective Hamiltonian for the composite system \bar{H}'_{AB} is additively separable, *i.e.*, $\bar{H}'_{AB} = \bar{H}'_A + \bar{H}'_B$.

Consider an excited state of the composite system A* + B with separable wavefunction $\Psi_{A^*B} = \Psi_{A^*} \Psi_B$. Our goal is to prove that the solutions of the EOM equation for the composite system (omitting the index α for clarity):

$$\bar{\mathbf{H}}'_{A+B} \mathbf{r}_{A+B} = \omega_{A+B} \mathbf{S}'_{A+B} \mathbf{r}_{A+B}, \quad (\text{B1})$$

contain all the solutions of the EOM problem for the isolated system A:

$$\bar{\mathbf{H}}'_A \mathbf{r}_A = \omega_A \mathbf{S}'_A \mathbf{r}_A. \quad (\text{B2})$$

To prove that EOM-ic-MRUCC satisfies this condition, it is sufficient to show that the Hamiltonian ($\bar{\mathbf{H}}'$) and metric (\mathbf{S}') matrices (in the original $\hat{\rho}$ basis) are block-diagonal, when we partition the operators into the three sets of excitations localized on A or B and excitations involving A and B.

Since the ground state reference is assumed to be separable, the original, linearly dependent, EOM operators basis involving orbitals from both subsystems are multiplicatively separable, that is, we can write an operator as $\hat{\rho}_{AB} = \tilde{\rho}_A \tilde{\rho}_B$, where $\tilde{\rho}_A$ and $\tilde{\rho}_B$ act only on A or B. For external excitations, these operators correspond to normal-ordered products $\{\hat{a}_{ij}^{ab\dots}\}_X$ while for internals they are projected operators of the form $\{\hat{a}_{uv\dots}^{xy\dots}\}_X |\Phi_X\rangle \langle \Phi_X|$ where $X = A$ or B denotes a restriction of the indices. As a consequence, these operators satisfy the killer condition when applied to the individual fragment reference states.

This property holds for the generalized normal-ordered operators since, for separable states, there are no cumulants involving orbitals from both A and B. Elements of the effective Hamiltonian within the A-B block can be shown to be null:

$$\begin{aligned} & \langle \Phi_0^A \Phi_0^B | [\hat{\rho}_A^\dagger, [\bar{H}'_A + \bar{H}'_B, \hat{\rho}_B]] | \Phi_0^A \Phi_0^B \rangle \\ &= \langle \Phi_0^A \Phi_0^B | [\hat{\rho}_A^\dagger, [\bar{H}'_A, \hat{\rho}_B]] | \Phi_0^A \Phi_0^B \rangle \\ & \quad + \underbrace{\langle \Phi_0^A \Phi_0^B | [\hat{\rho}_A^\dagger, [\bar{H}'_B, \hat{\rho}_B]] | \Phi_0^A \Phi_0^B \rangle}_{=0} \\ &= 0, \end{aligned} \quad (\text{B3})$$

where we used the fact that commutators of the form $[\hat{O}_A, \hat{O}_B]$ evaluate to zero since all contracted terms are multiplied by cumulants with indices that belong to both A and B.

Next, we consider the A/A+B block. In this case the matrix elements are also null:

$$\begin{aligned} & \langle \Phi_0^A \Phi_0^B | [\hat{\rho}_A^\dagger, [\bar{H}'_A + \bar{H}'_B, \hat{\rho}_{A+B}]] | \Phi_0^A \Phi_0^B \rangle \\ &= \langle \Phi_0^A \Phi_0^B | [\hat{\rho}_A^\dagger, [\bar{H}'_A, \hat{\rho}_{A+B}]] | \Phi_0^A \Phi_0^B \rangle \\ & \quad + \langle \Phi_0^A \Phi_0^B | [\hat{\rho}_A^\dagger, [\bar{H}'_B, \hat{\rho}_{A+B}]] | \Phi_0^A \Phi_0^B \rangle \\ &= \langle \Phi_0^A \Phi_0^B | \hat{\rho}_A^\dagger [\bar{H}'_A, \hat{\rho}_{A+B}] | \Phi_0^A \Phi_0^B \rangle \\ & \quad + \langle \Phi_0^A \Phi_0^B | \hat{\rho}_A^\dagger [\bar{H}'_B, \hat{\rho}_{A+B}] | \Phi_0^A \Phi_0^B \rangle \\ &= \langle \Phi_0^A | \hat{\rho}_A^\dagger \bar{H}'_A \tilde{\rho}_A | \Phi_0^A \rangle \underbrace{\langle \Phi_0^B | \tilde{\rho}_B | \Phi_0^B \rangle}_{=0} \\ & \quad - \langle \Phi_0^A | \hat{\rho}_A^\dagger \tilde{\rho}_A \bar{H}'_A | \Phi_0^A \rangle \underbrace{\langle \Phi_0^B | \tilde{\rho}_B | \Phi_0^B \rangle}_{=0} \\ & \quad + \langle \Phi_0^A | \hat{\rho}_A^\dagger \tilde{\rho}_A | \Phi_0^A \rangle \langle \Phi_0^B | \bar{H}'_B \tilde{\rho}_B | \Phi_0^B \rangle \\ & \quad - \langle \Phi_0^A | \hat{\rho}_A^\dagger \tilde{\rho}_A | \Phi_0^A \rangle \underbrace{\langle \Phi_0^B | \tilde{\rho}_B \bar{H}'_B | \Phi_0^B \rangle}_{=0}. \end{aligned} \quad (\text{B4})$$

In deriving this result, we have first used the killer condition (e.g., $\hat{\rho}_A^\dagger \Phi_0^A = 0$) to eliminate one of the commutators, then we decomposed the excitation operator from the A + B block as $\hat{\rho}_{AB} = \tilde{\rho}_A \tilde{\rho}_B$ separating terms in the expectation value into products of averages over A and B. Three of these terms are null due to the killer condition (first, second, and fourth terms), while the third term defines a necessary and sufficient condition for the energy

to be size extensive. This condition may be written as

$$\langle \Phi_0^A | \hat{\rho}_A^\dagger \tilde{\rho}_A | \Phi_0^A \rangle \langle \Phi_0^B | \hat{\rho}_B^\dagger \tilde{H}'_B | \Phi_0^B \rangle^* = 0, \quad (\text{B5})$$

and may be satisfied if one of the terms in the product is zero. Since $\langle \Phi_0^A | \hat{\rho}_A^\dagger \tilde{\rho}_A | \Phi_0^A \rangle$ is not generally guaranteed to be zero, the condition $\langle \Phi_0^B | \hat{\rho}_B^\dagger \tilde{H}'_B | \Phi_0^B \rangle = 0$ ultimately determines the size-intensivity property. This proof may be easily extended to the other blocks of the EOM Hamiltonian and the metric matrix.

APPENDIX C: Detailed derivation of the generalized normal-ordering transformation matrix

In this appendix, we derive the matrix \mathbf{G} that transforms the operator basis into generalized normal-ordered (GNO) operators. We focus here on the case of single and double excitations, with corresponding explicit relations for the GNO operators:

$$\{\hat{a}_q^p\} = \hat{a}_q^p - \gamma_q^p \quad (\text{C1})$$

$$\{\hat{a}_{rs}^{pq}\} = \hat{a}_{rs}^{pq} - P(pq)P(rs)\gamma_r^p\hat{a}_s^q + P(pq)P(rs)\gamma_r^p\gamma_s^q - \gamma_{rs}^{pq}, \quad (\text{C2})$$

where γ_q^p and γ_{rs}^{pq} are one- and two-body reduced density matrices (RDMs) of the reference state:

$$\gamma_q^p = \langle \Phi_0 | \hat{a}_p^\dagger \hat{a}_q | \Phi_0 \rangle, \quad (\text{C3})$$

$$\gamma_{rs}^{pq} = \langle \Phi_0 | \hat{a}_p^\dagger \hat{a}_q^\dagger \hat{a}_s \hat{a}_r | \Phi_0 \rangle, \quad (\text{C4})$$

and $P(pq)$ denotes the antisymmetric permutation operator, defined as:

$$P(pq)f(p, q) = f(p, q) - f(q, p). \quad (\text{C5})$$

Collecting these transformations into a matrix form naturally leads to a block matrix \mathbf{G} with the structure

$$\mathbf{G} = \begin{pmatrix} \mathbf{1} & \mathbf{G}_{01} & \mathbf{G}_{02} \\ \mathbf{0} & \mathbf{1} & \mathbf{G}_{12} \\ \mathbf{0} & \mathbf{0} & \mathbf{1} \end{pmatrix}, \quad (\text{C6})$$

where the identity blocks $\mathbf{1}$ imply that operators within a given excitation manifold (reference, singles, or doubles) remain unchanged under the GNO transformation. The nontrivial transformations appear in the off-diagonal blocks:

$$(G_{12})_{a,jk}^{i,bc} = \delta_k^i (\delta_b^a \gamma_c^j - \delta_c^a \gamma_b^j) + \delta_j^i (\delta_c^a \gamma_b^k - \delta_b^a \gamma_c^k), \quad (\text{C7})$$

$$(G_{01})_v^u = -\gamma_v^u, \quad (\text{C8})$$

$$(G_{02})_{xy}^{uv} = -2\gamma_y^u \gamma_x^v + 2\gamma_x^u \gamma_y^v - \gamma_{xy}^{uv}. \quad (\text{C9})$$

Here, the superscripts and subscripts on the tensor elements of \mathbf{G} track the transformation from one sector (e.g., reference, denoted by 0) to another (e.g., singles or doubles). For instance, $(G_{01})_v^u$ represents the part of the transformation matrix that couples the reference to singles.

REFERENCES

- 1 J. B. Foresman, M. Head-Gordon, J. A. Pople, and M. J. Frisch, "Toward a systematic molecular orbital theory for excited states," *J. Phys. Chem.* **96**, 135–149 (1992).
- 2 M. E. Casida, "Time-dependent density functional response theory for molecules," in *Recent Advances In Density Functional Methods: (Part I)* (1995) pp. 155–192.
- 3 F. Furche and R. Ahlrichs, "Adiabatic time-dependent density functional methods for excited state properties," *J. Chem. Phys.* **117**, 7433–7447 (2002).
- 4 J. Čížek, "On the Correlation Problem in Atomic and Molecular Systems. Calculation of Wavefunction Components in Ursell-Type Expansion Using Quantum-Field Theoretical Methods," *J. Chem. Phys.* **45**, 4256–4266 (1966).
- 5 T. D. Crawford and H. F. Schaefer III, "An Introduction to Coupled Cluster Theory for Computational Chemists," *Rev. Comput. Chem.* **14**, 33–136 (2000).
- 6 R. J. Bartlett and M. Musial, "Coupled-cluster theory in quantum chemistry," *Rev. Mod. Phys.* **79**, 291–352 (2007).
- 7 H. J. Monkhorst, "Calculation of properties with the coupled-cluster method," *Int. J. Quantum Chem.* **12**, 421–432 (1977).
- 8 D. Mukherjee and P. Mukherjee, "A response-function approach to the direct calculation of the transition-energy in a multiple-cluster expansion formalism," *Chem. Phys.* **39**, 325–335 (1979).
- 9 E. Dalgaard and H. J. Monkhorst, "Some aspects of the time-dependent coupled-cluster approach to dynamic response functions," *Phys. Rev. A* **28**, 1217 (1983).
- 10 H. Koch and P. Jørgensen, "Coupled cluster response functions," *J. Chem. Phys.* **93**, 3333 (1990).
- 11 D. J. Rowe, "Equations-of-Motion Method and the Extended Shell Model," *Rev. Mod. Phys.* **40**, 153–166 (1968).
- 12 J. Geertsen, M. Rittby, and R. J. Bartlett, "The equation-of-motion coupled-cluster method: Excitation energies of be and co," *Chem. Phys. Lett.* **164**, 57–62 (1989).
- 13 J. F. Stanton and R. J. Bartlett, "The equation of motion coupled-cluster method. a systematic biorthogonal approach to molecular excitation energies, transition probabilities, and excited state properties," *J. Chem. Phys.* **98**, 7029–7039 (1993).
- 14 D. Mukhopadhyay, S. Mukhopadhyay, R. Chaudhuri, and D. Mukherjee, "Aspects of separability in the coupled cluster based direct methods for energy differences," *Theor. Chim. Acta* **80**, 441–467 (1991).
- 15 M. Nooijen and R. J. Bartlett, "Description of core-excitation spectra by the open-shell electron-attachment equation-of-motion coupled cluster method," *J. Chem. Phys.* **102**, 6735–6756 (1995).
- 16 J. D. Watts and R. J. Bartlett, "Iterative and non-iterative triple excitation corrections in coupled-cluster methods for excited electronic states: the eom-ccsd-t3 and eom-ccsd (t) methods," *Chem. Phys. Lett.* **258**, 581–588 (1996).
- 17 A. Y. Sokolov, "Multi-reference algebraic diagrammatic construction theory for excited states: General formulation and first-order implementation," *J. Chem. Phys.* **149** (2018).
- 18 H. Nakatsuji, "Cluster expansion of the wavefunction. calculation of electron correlations in ground and excited states by sac and sac ci theories," *Chem. Phys. Lett.* **67**, 334–342 (1979).
- 19 L. Meissner, A. Balková, and R. J. Bartlett, "Multiple solutions of the single-reference coupled-cluster method," *Chem. Phys. Lett.* **212**, 177–184 (1993).
- 20 K. Jankowski, K. Kowalski, and P. Jankowski, "Multiple solutions of the single-reference coupled-cluster equations. I. H4 model revisited," *Int. J. Quantum Chem.* **50**, 353–367 (1994).
- 21 K. Jankowski, K. Kowalski, and P. Jankowski, "Multiple solutions of the single-reference coupled-cluster equations. II. Alternative reference states," *Int. J. Quantum Chem.* **53**, 501–514 (1995).
- 22 K. Kowalski and K. Jankowski, "Towards Complete Solutions to Systems of Nonlinear Equations of Many-Electron Theories," *Phys. Rev. Lett.* **81**, 1195–1198 (1998).

- ²³K. Jankowski and K. Kowalski, "Physical and mathematical content of coupled-cluster equations. II. On the origin of irregular solutions and their elimination via symmetry adaptation," *J. Chem. Phys.* **110**, 9345–9352 (1999).
- ²⁴K. Jankowski and K. Kowalski, "Physical and mathematical content of coupled-cluster equations. III. Model studies of dissociation processes for various reference states," *J. Chem. Phys.* **111**, 2940–2951 (1999).
- ²⁵P. Piecuch and K. Kowalski, "In Search of the Relationship between Multiple Solutions Characterizing Coupled-Cluster Theories," in *Computational Chemistry: Reviews of Current Trends*, Computational Chemistry: Reviews of Current Trends, Vol. Volume 5 (World Scientific, 2000) pp. 1–104.
- ²⁶N. J. Mayhall and K. Raghavachari, "Multiple Solutions to the Single-Reference CCSD Equations for NiH," *J. Chem. Theory Comput.* **6**, 2714–2720 (2010).
- ²⁷J. Lee, D. W. Small, and M. Head-Gordon, "Excited states via coupled cluster theory without equation-of-motion methods: Seeking higher roots with application to doubly excited states and double core hole states," *J. Chem. Phys.* **151**, 214103 (2019).
- ²⁸F. Kossoski, A. Marie, A. Scemama, M. Caffarel, and P.-F. Loos, "Excited States from State-Specific Orbital-Optimized Pair Coupled Cluster," *J. Chem. Theory Comput.* **17**, 4756–4768 (2021).
- ²⁹Y. Damour, A. Scemama, D. Jacquemin, F. Kossoski, and P.-F. Loos, "State-Specific Coupled-Cluster Methods for Excited States," *J. Chem. Theory Comput.* **20**, 4129–4145 (2024).
- ³⁰M. Hanrath, "On the concepts of connectivity, separability, and consistency: An illustration by partitioned diagrams and numerical probing," *Chem. Phys.* **356**, 31–38 (2009).
- ³¹I. Hubač and P. Neogrady, "Size-consistent brillouin-wigner perturbation theory with an exponentially parametrized wave function: Brillouin-wigner coupled-cluster theory," *Phys. Rev. A* **50**, 4558 (1994).
- ³²J. Mášik, I. Hubač, and P. Mach, "Single-root multireference brillouin-wigner coupled-cluster theory: Applicability to the f 2 molecule," *J. Chem. Phys.* **108**, 6571–6579 (1998).
- ³³U. S. Mahapatra, B. Datta, and D. Mukherjee, "A state-specific multi-reference coupled cluster formalism with molecular applications," *Mol. Phys.* **94**, 157–171 (1998).
- ³⁴U. S. Mahapatra, B. Datta, and D. Mukherjee, "A size-consistent state-specific multireference coupled cluster theory: Formal developments and molecular applications," *J. Chem. Phys.* **110**, 6171–6188 (1999).
- ³⁵U. S. Mahapatra and S. Chattopadhyay, "Potential energy surface studies via a single root multireference coupled cluster theory," *J. Chem. Phys.* **133** (2010).
- ³⁶U. S. Mahapatra and S. Chattopadhyay, "Evaluation of the performance of single root multireference coupled cluster method for ground and excited states, and its application to geometry optimization," *J. Chem. Phys.* **134** (2011).
- ³⁷T.-C. Jagau and J. Gauss, "Linear-response theory for mukherjee's multireference coupled-cluster method: Excitation energies," *J. Chem. Phys.* **137** (2012).
- ³⁸T.-C. Jagau and J. Gauss, "Linear-response theory for mukherjee's multireference coupled-cluster method: Static and dynamic polarizabilities," *J. Chem. Phys.* **137** (2012).
- ³⁹B. Jeziorski and H. J. Monkhorst, "Coupled-cluster method for multideterminantal reference states," *Phys. Rev. A* **24**, 1668–1681 (1981).
- ⁴⁰D. Mukherjee, R. K. Moitra, and A. Mukhopadhyay, "Correlation problem in open-shell atoms and molecules: A non-perturbative linked cluster formulation," *Mol. Phys.* **30**, 1861–1888 (1975).
- ⁴¹A. Banerjee and J. Simons, "The coupled-cluster method with a multiconfiguration reference state," *Int. J. Quantum Chem.* **19**, 207–216 (1981).
- ⁴²A. Banerjee and J. Simons, "Applications of multiconfigurational coupled-cluster theory," *J. Chem. Phys.* **76**, 4548–4559 (1982).
- ⁴³F. A. Evangelista and J. Gauss, "An orbital-invariant internally contracted multireference coupled cluster approach," *J. Chem. Phys.* **134** (2011), 10.1063/1.3559149.
- ⁴⁴M. Hanauer and A. Köhn, "Pilot applications of internally contracted multireference coupled cluster theory, and how to choose the cluster operator properly," *J. Chem. Phys.* **134** (2011), 10.1063/1.3592786.
- ⁴⁵M. Hanauer and A. Köhn, "Communication: Restoring full size extensivity in internally contracted multireference coupled cluster theory," *J. Chem. Phys.* **137** (2012), 10.1063/1.4757728.
- ⁴⁶D. Datta, L. Kong, and M. Nooijen, "A state-specific partially internally contracted multireference coupled cluster approach," *J. Chem. Phys.* **134** (2011).
- ⁴⁷T. Yanai and G. K. Chan, "Canonical transformation theory for multireference problems," *J. Chem. Phys.* **124** (2006).
- ⁴⁸T. Yanai and G. K. Chan, "Canonical transformation theory from extended normal ordering," *J. Chem. Phys.* **127** (2007).
- ⁴⁹R. Feldmann and M. Reiher, "Renormalized internally contracted multireference coupled cluster with perturbative triples," *J. Chem. Theory Comput.* (2024).
- ⁵⁰D. A. Mazziotti, "Anti-hermitian contracted schrödinger equation: Direct determination of the two-electron reduced density matrices of many-electron molecules," *Phys. Rev. Lett.* **97**, 143002 (2006).
- ⁵¹D. A. Mazziotti, "Anti-hermitian part of the contracted schrödinger equation for the direct calculation of two-electron reduced density matrices," *Phys. Rev. A* **75**, 022505 (2007).
- ⁵²L. Greenman and D. A. Mazziotti, "Electronic excited-state energies from a linear response theory based on the ground-state two-electron reduced density matrix," *J. Chem. Phys.* **128** (2008).
- ⁵³D. Datta and M. Nooijen, "Multireference equation-of-motion coupled cluster theory," *J. Chem. Phys.* **137** (2012), 10.1063/1.4766361.
- ⁵⁴P. K. Samanta, D. Mukherjee, M. Hanauer, and A. Köhn, "Excited states with internally contracted multireference coupled-cluster linear response theory," *J. Chem. Phys.* **140** (2014).
- ⁵⁵S. Thomas, F. Hampe, S. Stopkiewicz, and J. Gauss, "Complex ground-state and excitation energies in coupled-cluster theory," *Mol. Phys.* **119**, e1968056 (2021).
- ⁵⁶W. Kutzelnigg, "Pair Correlation Theories," in *Methods of Electronic Structure Theory*, edited by H. F. Schaefer (Springer US, Boston, MA, 1977) pp. 129–188.
- ⁵⁷S. A. Kucharski and R. J. Bartlett, "Hilbert space multireference coupled-cluster methods. i. the single and double excitation model," *J. Chem. Phys.* **95**, 8227–8238 (1991).
- ⁵⁸W. Kutzelnigg and S. Koch, "Quantum chemistry in Fock space. II. Effective Hamiltonians in Fock space," *J. Chem. Phys.* **79**, 4315–4335 (1983).
- ⁵⁹W. Kutzelnigg, "Quantum chemistry in Fock space. III. Particle-hole formalism," *J. Chem. Phys.* **80**, 822–830 (1984).
- ⁶⁰R. J. Bartlett, S. A. Kucharski, and J. Noga, "Alternative coupled-cluster ansätze II. The unitary coupled-cluster method," *Chem. Phys. Lett.* **155**, 133–140 (1989).
- ⁶¹P. G. Szalay, M. Nooijen, and R. J. Bartlett, "Alternative ansätze in single reference coupled-cluster theory. III. A critical analysis of different methods," *J. Chem. Phys.* **103**, 281–298 (1995).
- ⁶²K. Majee, S. Chakraborty, T. Mukhopadhyay, M. K. Nayak, and A. K. Dutta, "A reduced cost four-component relativistic unitary coupled cluster method for atoms and molecules," *J. Chem. Phys.* **161**, 034101 (2024).
- ⁶³B. Cooper and P. J. Knowles, "Benchmark studies of variational, unitary and extended coupled cluster methods," *J. Chem. Phys.* **133**, 234102 (2010).
- ⁶⁴F. A. Evangelista, "Alternative single-reference coupled cluster approaches for multireference problems: The simpler, the better," *J. Chem. Phys.* **134** (2011), 10.1063/1.3598471.
- ⁶⁵G. Harsha, T. Shiozaki, and G. E. Scuseria, "On the difference

- between variational and unitary coupled cluster theories,” *J. Chem. Phys.* **148**, 044107 (2018).
- ⁶⁶M. Hodecker, D. R. Rehn, and A. Dreuw, “Hermitian second-order methods for excited electronic states: Unitary coupled cluster in comparison with algebraic–diagrammatic construction schemes,” *J. Chem. Phys.* **152**, 094106 (2020).
- ⁶⁷J. Tölle and G. Kin-Lic Chan, “Exact relationships between the GW approximation and equation-of-motion coupled-cluster theories through the quasi-boson formalism,” *J. Chem. Phys.* **158**, 124123 (2023).
- ⁶⁸M. Hodecker and A. Dreuw, “Unitary coupled cluster ground- and excited-state molecular properties,” *J. Chem. Phys.* **153**, 084112 (2020).
- ⁶⁹J. Liu, A. Asthana, L. Cheng, and D. Mukherjee, “Unitary coupled-cluster based self-consistent polarization propagator theory: A third-order formulation and pilot applications,” *J. Chem. Phys.* **148**, 244110 (2018).
- ⁷⁰J. Liu and L. Cheng, “Unitary coupled-cluster based self-consistent polarization propagator theory: A quadratic unitary coupled-cluster singles and doubles scheme,” *J. Chem. Phys.* **155**, 174102 (2021).
- ⁷¹A. G. Taube and R. J. Bartlett, “New perspectives on unitary coupled-cluster theory,” *Int. J. Quantum Chem.* **106**, 3393–3401 (2006).
- ⁷²W. Kutzelnigg, “Error analysis and improvements of coupled-cluster theory,” *Theor. Chim. Acta* **80**, 349–386 (1991).
- ⁷³I. M. Mazin and A. Y. Sokolov, “Multireference algebraic diagrammatic construction theory for excited states: Extended second-order implementation and benchmark,” *J. Chem. Theory Comput.* **17**, 6152–6165 (2021).
- ⁷⁴K. Chatterjee and A. Y. Sokolov, “Second-order multireference algebraic diagrammatic construction theory for photoelectron spectra of strongly correlated systems,” *J. Chem. Theory Comput.* **15**, 5908–5924 (2019).
- ⁷⁵K. Chatterjee and A. Y. Sokolov, “Extended second-order multireference algebraic diagrammatic construction theory for charged excitations,” *J. Chem. Theory Comput.* **16**, 6343–6357 (2020).
- ⁷⁶I. M. Mazin and A. Y. Sokolov, “Core-excited states and x-ray absorption spectra from multireference algebraic diagrammatic construction theory,” *J. Chem. Theory Comput.* **19**, 4991–5006 (2023).
- ⁷⁷C. E. de Moura and A. Y. Sokolov, “Efficient spin-adapted implementation of multireference algebraic diagrammatic construction theory. i. core-ionized states and x-ray photoelectron spectra,” *J. Phys. Chem. A* **128**, 5816–5831 (2024).
- ⁷⁸A. Peruzzo, J. McClean, P. Shadbolt, M.-H. Yung, X.-Q. Zhou, P. J. Love, A. Aspuru-Guzik, and J. L. O’Brien, “A variational eigenvalue solver on a photonic quantum processor,” *Nat. Commun.* **5**, 4213 (2014).
- ⁷⁹A. Aspuru-Guzik, A. D. Dutoi, P. J. Love, and M. Head-Gordon, “Simulated Quantum Computation of Molecular Energies,” *Science* **309**, 1704–1707 (2005).
- ⁸⁰J. R. McClean, M. E. Kimchi-Schwartz, J. Carter, and W. A. de Jong, “Hybrid quantum-classical hierarchy for mitigation of decoherence and determination of excited states,” *Phys. Rev. A* **95**, 042308 (2017).
- ⁸¹M. Motta, C. Sun, A. T. K. Tan, M. J. O’Rourke, E. Ye, A. J. Minnich, F. G. S. L. Brandt, and G. K.-L. Chan, “Determining eigenstates and thermal states on a quantum computer using quantum imaginary time evolution,” *Nat. Phys.* **16**, 205–210 (2020).
- ⁸²N. H. Stair and F. A. Evangelista, “Simulating Many-Body Systems with a Projective Quantum Eigensolver,” *PRX Quantum* **2**, 030301 (2021).
- ⁸³S. E. Smart and D. A. Mazziotti, “Quantum Solver of Contracted Eigenvalue Equations for Scalable Molecular Simulations on Quantum Computing Devices,” *Phys. Rev. Lett.* **126**, 070504 (2021).
- ⁸⁴C. L. Benavides-Riveros, Y. Wang, S. Warren, and D. A. Mazziotti, “Quantum simulation of excited states from parallel contracted quantum eigensolvers,” *New J. Phys.* **26**, 033020 (2024).
- ⁸⁵M. Otten, M. R. Hermes, R. Pandharkar, Y. Alexeev, S. K. Gray, and L. Gagliardi, “Localized Quantum Chemistry on Quantum Computers,” *J. Chem. Theory Comput.* **18**, 7205–7217 (2022).
- ⁸⁶Q.-X. Xie, Y. Song, and Y. Zhao, “Power of the Sine Hamiltonian Operator for Estimating the Eigenstate Energies on Quantum Computers,” *J. Chem. Theory Comput.* **18**, 7586–7602 (2022).
- ⁸⁷J. Wen, Z. Wang, C. Chen, J. Xiao, H. Li, L. Qian, Z. Huang, H. Fan, S. Wei, and G. Long, “A full circuit-based quantum algorithm for excited-states in quantum chemistry,” *Quantum* **8**, 1219 (2024).
- ⁸⁸N. V. Tkachenko, L. Cincio, A. I. Boldyrev, S. Tretiak, P. A. Dub, and Y. Zhang, “Quantum Davidson algorithm for excited states,” *Quantum Sci. Technol.* **9**, 035012 (2024).
- ⁸⁹H. R. Grimsley and F. A. Evangelista, “Challenging Excited States from Adaptive Quantum Eigensolvers: Subspace Expansions vs. State-Averaged Strategies,” (2024), arXiv:2409.11210.
- ⁹⁰P. J. Ollitrault, A. Kandala, C.-F. Chen, P. K. Barkoutsos, A. Mezzacapo, M. Pistoia, S. Sheldon, S. Woerner, J. M. Gambetta, and I. Tavernelli, “Quantum equation of motion for computing molecular excitation energies on a noisy quantum processor,” *pr* **2**, 043140 (2020).
- ⁹¹A. Asthana, A. Kumar, V. Abraham, H. Grimsley, Y. Zhang, L. Cincio, S. Tretiak, P. A. Dub, S. E. Economou, E. Barnes, and N. J. Mayhall, “Quantum self-consistent equation-of-motion method for computing molecular excitation energies, ionization potentials, and electron affinities on a quantum computer,” *Chem. Sci.* **14**, 2405–2418 (2023).
- ⁹²E. R. Kjellgren, P. Reinholdt, K. M. Ziem, S. P. A. Sauer, S. Coriani, and J. Kongsted, “Divergences in classical and quantum linear response and equation of motion formulations,” *J. Chem. Phys.* **161**, 124112 (2024).
- ⁹³K. M. Ziem, E. R. Kjellgren, S. P. A. Sauer, J. Kongsted, and S. Coriani, “Understanding and mitigating noise in molecular quantum linear response for spectroscopic properties on quantum computers,” (2024), arXiv:2408.09308.
- ⁹⁴Y. Kim and A. I. Krylov, “Two Algorithms for Excited-State Quantum Solvers: Theory and Application to EOM-UCCSD,” *J. Phys. Chem. A* **127**, 6552–6566 (2023).
- ⁹⁵A. Kumar, A. Asthana, V. Abraham, T. D. Crawford, N. J. Mayhall, Y. Zhang, L. Cincio, S. Tretiak, and P. A. Dub, “Quantum Simulation of Molecular Response Properties in the NISQ Era,” *J. Chem. Theory Comput.* **19**, 9136–9150 (2023).
- ⁹⁶M. D. Prasad, S. Pal, and D. Mukherjee, “Some aspects of self-consistent propagator theories,” *Phys. Rev. A* **31**, 1287 (1985).
- ⁹⁷B. Datta, D. Mukhopadhyay, and D. Mukherjee, “Consistent propagator theory based on the extended coupled-cluster parametrization of the ground state,” *Phys. Rev. A* **47**, 3632 (1993).
- ⁹⁸H. R. Grimsley, S. E. Economou, E. Barnes, and N. J. Mayhall, “An adaptive variational algorithm for exact molecular simulations on a quantum computer,” *Nat. Commun.* **10**, 3007 (2019).
- ⁹⁹K. M. Ziem, E. R. Kjellgren, P. Reinholdt, P. W. Jensen, S. P. Sauer, J. Kongsted, and S. Coriani, “Which options exist for nisq-friendly linear response formulations?” *J. Chem. Theory Comput.* **20**, 3551–3565 (2024).
- ¹⁰⁰P. W. K. Jensen, E. R. Kjellgren, P. Reinholdt, K. M. Ziem, S. Coriani, J. Kongsted, and S. P. A. Sauer, “Quantum Equation of Motion with Orbital Optimization for Computing Molecular Properties in Near-Term Quantum Computing,” *J. Chem. Theory Comput.* **20**, 3613–3625 (2024).
- ¹⁰¹P. Reinholdt, E. R. Kjellgren, J. H. Fuglsbjerg, K. M. Ziem, S. Coriani, S. P. A. Sauer, and J. Kongsted, “Subspace Methods for the Simulation of Molecular Response Properties on a Quantum Computer,” *J. Chem. Theory Comput.* **20**, 3729–3740 (2024).
- ¹⁰²T. J. von Buchwald, K. M. Ziem, E. R. Kjellgren, S. P. A.

- Sauer, J. Kongsted, and S. Coriani, "Reduced Density Matrix Formulation of Quantum Linear Response," *J. Chem. Theory Comput.* **20**, 7093–7101 (2024).
- ¹⁰³C. L. Benavides-Riveros, Y. Wang, S. Warren, and D. A. Mazziotti, "Quantum simulation of excited states from parallel contracted quantum eigensolvers," *njp* **26**, 033020 (2024).
- ¹⁰⁴Y. Wang and D. A. Mazziotti, "Electronic excited states from a variance-based contracted quantum eigensolver," *Phys. Rev. A* **108**, 022814 (2023).
- ¹⁰⁵F. A. Evangelista, "Alternative single-reference coupled cluster approaches for multireference problems: The simpler, the better," *J. Chem. Phys.* **134**, 224102 (2011).
- ¹⁰⁶Z. Chen and M. R. Hoffmann, "Orbitally invariant internally contracted multireference unitary coupled cluster theory and its perturbative approximation: Theory and test calculations of second order approximation," *J. Chem. Phys.* **137** (2012), 10.1063/1.4731634.
- ¹⁰⁷F. A. Evangelista, "A driven similarity renormalization group approach to quantum many-body problems," *J. Chem. Phys.* **141** (2014).
- ¹⁰⁸C. Li and F. A. Evangelista, "Multireference driven similarity renormalization group: A second-order perturbative analysis," *J. Chem. Theory Comput.* **11**, 2097–2108 (2015).
- ¹⁰⁹C. Li and F. A. Evangelista, "Driven similarity renormalization group: Third-order multireference perturbation theory," *J. Chem. Phys.* **146** (2017).
- ¹¹⁰C. Li and F. A. Evangelista, "Towards numerically robust multireference theories: The driven similarity renormalization group truncated to one- and two-body operators," *J. Chem. Phys.* **144** (2016).
- ¹¹¹C. Li and F. A. Evangelista, "Multireference theories of electron correlation based on the driven similarity renormalization group," *Annu. Rev. Phys. Chem.* **70**, 245–273 (2019).
- ¹¹²D. Mukherjee, "Normal ordering and a Wick-like reduction theorem for fermions with respect to a multi-determinantal reference state," *Chem. Phys. Lett.* **274**, 561–566 (1997).
- ¹¹³W. Kutzelnigg and D. Mukherjee, "Normal order and extended Wick theorem for a multiconfiguration reference wave function," *J. Chem. Phys.* **107**, 432–449 (1997).
- ¹¹⁴L. Kong, M. Nooijen, and D. Mukherjee, "An algebraic proof of generalized Wick theorem," *J. Chem. Phys.* **132**, 234107 (2010).
- ¹¹⁵P.-O. Löwdin, "On the nonorthogonality problem," in *Adv. Quantum Chem.*, Vol. 5 (1970) pp. 185–199.
- ¹¹⁶H.-J. Werner and P. J. Knowles, "An efficient internally contracted multiconfiguration-reference configuration interaction method," *J. Chem. Phys.* **89**, 5803–5814 (1988).
- ¹¹⁷K. Andersson, P. A. Malmqvist, B. O. Roos, A. J. Sadlej, and K. Wolinski, "Second-order perturbation theory with a cascf reference function," *J. Phys. Chem.* **94**, 5483–5488 (1990).
- ¹¹⁸F. A. Evangelista, M. Hanauer, A. Köhn, and J. Gauss, "A sequential transformation approach to the internally contracted multireference coupled cluster method," *J. Chem. Phys.* **136** (2012).
- ¹¹⁹F. A. Evangelista, G. K. Chan, and G. E. Scuseria, "Exact parameterization of fermionic wave functions via unitary coupled cluster theory," *J. Chem. Phys.* **151** (2019).
- ¹²⁰O. Goscinski and B. Weiner, "The role of algebraic formulations of approximate green's functions for systems with a finite number of electrons," *Phys. Scr.* **21**, 385 (1980).
- ¹²¹B. Weiner and O. Goscinski, "Self-consistent approximation to the polarization propagator," *Int. J. Quantum Chem.* **18**, 1109–1131 (1980).
- ¹²²Z. Szekeres, Á. Szabados, M. Kállay, and P. R. Surján, "On the "killer condition" in the equation-of-motion method: ionization potentials from multi-reference wave functions," *Phys. Chem. Chem. Phys.* **3**, 696–701 (2001).
- ¹²³P.-O. Löwdin, "Some aspects on the hamiltonian and liouvillean formalism, the special propagator methods, and the equation of motion approach," in *Adv. Quantum Chem.*, Vol. 17 (1985) pp. 285–334.
- ¹²⁴W. Kutzelnigg and D. Mukherjee, "Time-independent theory of one-particle green's functions," *J. Chem. Phys.* **90**, 5578–5594 (1989).
- ¹²⁵Y. Fan, J. Liu, Z. Li, and J. Yang, "Equation-of-Motion Theory to Calculate Accurate Band Structures with a Quantum Computer," *npj* **12**, 8833–8840 (2021).
- ¹²⁶J. Liu, Y. Fan, Z. Li, and J. Yang, "Quantum algorithms for electronic structures: Basis sets and boundary conditions," *csr* **51**, 3263–3279 (2022).
- ¹²⁷F. A. Evangelista, C. Li, P. Verma, K. P. Hannon, J. B. Schriber, T. Zhang, C. Cai, S. Wang, N. He, N. H. Stair, *et al.*, "Forte: A suite of advanced multireference quantum chemistry methods," *J. Chem. Phys.* **161** (2024).
- ¹²⁸D. G. Smith, L. A. Burns, A. C. Simmonett, R. M. Parrish, M. C. Schieber, R. Galvelis, P. Kraus, H. Kruse, R. Di Remigio, A. Alenaizan, *et al.*, "Psi4 1.4: Open-source software for high-throughput quantum chemistry," *J. Chem. Phys.* **152** (2020), 10.1063/5.0006002.
- ¹²⁹G. D. Purvis III and R. J. Bartlett, "A full coupled-cluster singles and doubles model: The inclusion of disconnected triples," *J. Chem. Phys.* **76**, 1910–1918 (1982).
- ¹³⁰G. D. Purvis III, R. Shepard, F. B. Brown, and R. J. Bartlett, "C2v insertion pathway for beh2: A test problem for the coupled-cluster single and double excitation model," *Int. J. Quantum Chem.* **23**, 835–845 (1983).
- ¹³¹M. R. Hoffmann and J. Simons, "A unitary multiconfigurational coupled-cluster method: Theory and applications," *J. Chem. Phys.* **88**, 993–1002 (1988).
- ¹³²R. J. Gdanitz and R. Ahlrichs, "The averaged coupled-pair functional (acpf): A size-extensive modification of mrci (sd)," *Chem. Phys. Lett.* **143**, 413–420 (1988).
- ¹³³S. B. Sharp and G. I. Gellene, " σ bond activation by cooperative interaction with n s2 atoms: Be+ n h2, n= 1- 3," *J. Phys. Chem. A* **104**, 10951–10957 (2000).
- ¹³⁴M. Kállay, P. G. Szalay, and P. R. Surján, "A general state-selective multireference coupled-cluster algorithm," *J. Chem. Phys.* **117**, 980–990 (2002).
- ¹³⁵P. Ruttink, J. Van Lenthe, and P. Todorov, "Multireference coupled electron-pair approximations to the multireference coupled cluster method. the mr-cepal method," *Mol. Phys.* **103**, 2497–2506 (2005).
- ¹³⁶J. Pittner, H. V. Gonzalez, R. J. Gdanitz, and P. Čársky, "The performance of the multireference brillouin–wigner coupled cluster singles and doubles method on the insertion of be into h2," *Chem. Phys. Lett.* **386**, 211–215 (2004).
- ¹³⁷D. I. Lyakh, V. V. Ivanov, and L. Adamowicz, "Multireference state-specific coupled cluster approach with the cas reference: inserting be into h2," *Theor. Chim. Acta* **116**, 427–433 (2006).
- ¹³⁸S. Das, D. Mukherjee, and M. Kállay, "Full implementation and benchmark studies of mukherjee's state-specific multireference coupled-cluster ansatz," *J. Chem. Phys.* **132** (2010).
- ¹³⁹P. G. Szalay and R. J. Bartlett, "Approximately extensive modifications of the multireference configuration interaction method: A theoretical and practical analysis," *J. Chem. Phys.* **103**, 3600–3612 (1995).
- ¹⁴⁰C. W. Bauschlicher Jr and P. R. Taylor, "Benchmark full configuration-interaction calculations on h2o, f, and f-," *J. Chem. Phys.* **85**, 2779–2783 (1986).
- ¹⁴¹J. Olsen, P. Jørgensen, H. Koch, A. Balkova, and R. J. Bartlett, "Full configuration–interaction and state of the art correlation calculations on water in a valence double-zeta basis with polarization functions," *J. Chem. Phys.* **104**, 8007–8015 (1996).
- ¹⁴²S. Li, J. Ma, and Y. Jiang, "Pair-correlated coupled cluster theory: An alternative multireference coupled cluster method," *J. Chem. Phys.* **118**, 5736–5745 (2003).
- ¹⁴³U. S. Mahapatra, S. Chattopadhyay, and R. K. Chaudhuri, "Molecular applications of state-specific multireference perturbation theory to hf, h2o, h2s, c2, and n2 molecules," *J. Chem. Phys.* **129** (2008).

- ¹⁴⁴S. Li, J. P. Misiewicz, and F. A. Evangelista, “Intruder-free cumulant-truncated driven similarity renormalization group second-order multireference perturbation theory,” *J. Chem. Phys.* **159** (2023).
- ¹⁴⁵M. Saitow, Y. Kurashige, and T. Yanai, “Multireference configuration interaction theory using cumulant reconstruction with internal contraction of density matrix renormalization group wave function,” *J. Chem. Phys.* **139** (2013).
- ¹⁴⁶S. Li, “Eom-ic-mrcc,” <https://github.com/shuhangli98/EOM-ic-MRUCC> (2024).
- ¹⁴⁷K. Brueckner, “Many-body problem for strongly interacting particles. ii. linked cluster expansion,” *Phys. Rev.* **100**, 36 (1955).
- ¹⁴⁸N. Hugenholtz, “Perturbation theory of large quantum systems,” *Physica* **23**, 481–532 (1957).
- ¹⁴⁹J. A. Pople, J. S. Binkley, and R. Seeger, “Theoretical models incorporating electron correlation,” *Int. J. Quantum Chem.* **10**, 1–19 (1976).
- ¹⁵⁰R. J. Bartlett, “Many-body perturbation theory and coupled cluster theory for electron correlation in molecules,” *Annu. Rev. Phys. Chem.* **32**, 359–401 (1981).
- ¹⁵¹A. Köhn, J. A. Black, Y. A. Aoto, and M. Hanauer, “Improved and simplified orthogonalisation scheme and connected triples correction within the internally contracted multireference coupled-cluster method,” *Mol. Phys.* **118**, e1743889 (2020).

Supplementary Information:
**Equation-of-motion internally contracted multireference unitary coupled-cluster
theory**

Shuhang Li^{1,*}, Zijun Zhao¹, and Francesco A. Evangelista^{1,*}

¹*Department of Chemistry and Cherry Emerson Center for Scientific Computation,
Emory University, Atlanta, Georgia 30322, USA*

* E-mails: shuhang.li@emory.edu, francesco.evangelista@emory.edu.

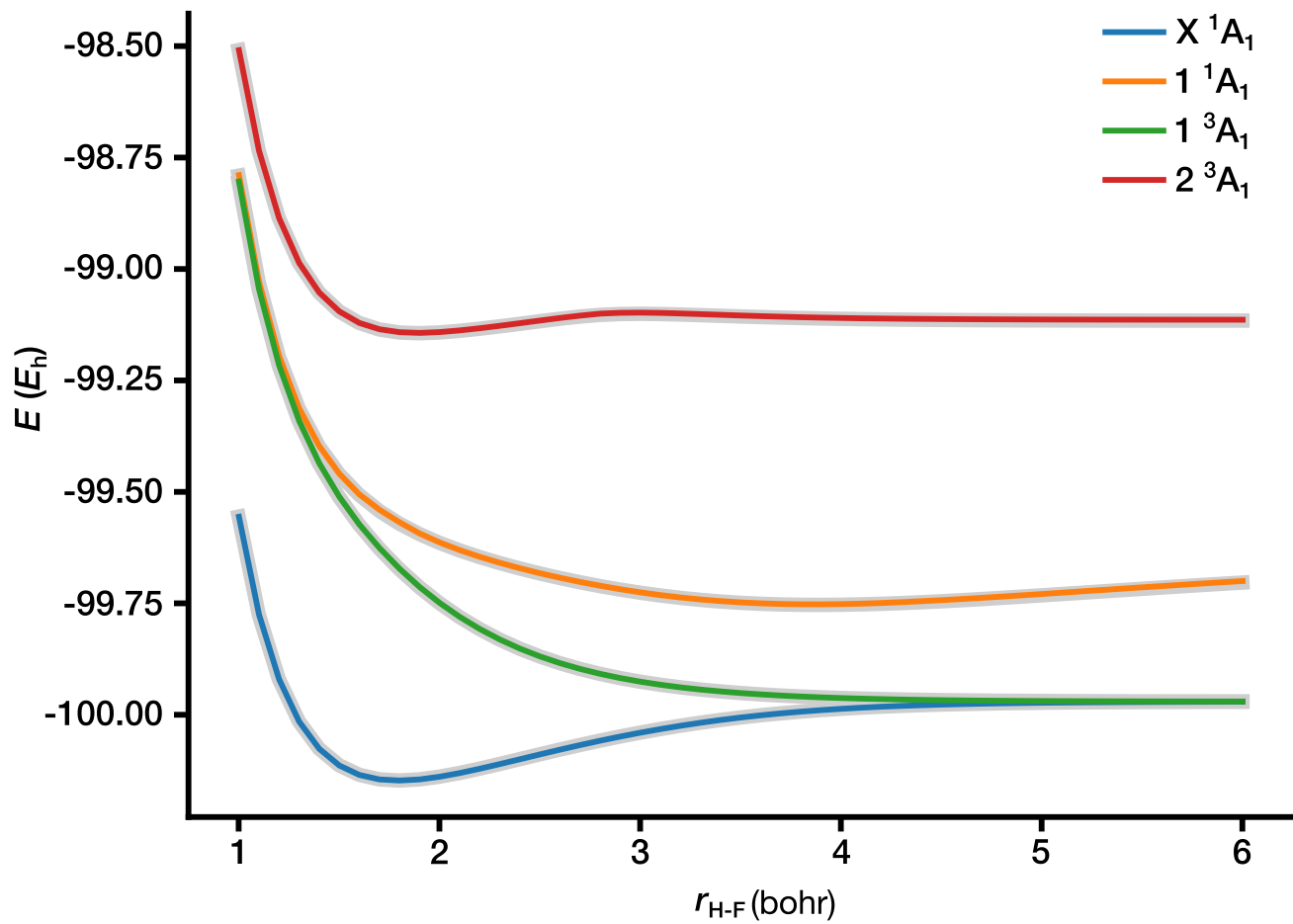


FIG. S1. Potential energy curves of FCI (gray) and EOM-ic-MRUCCSD (colored) for the X^1A_1 , 1^1A_1 , 1^3A_1 , and 2^3A_1 states of the HF molecule as a function of the bond distance ($r_{\text{H-F}}$ in \AA).

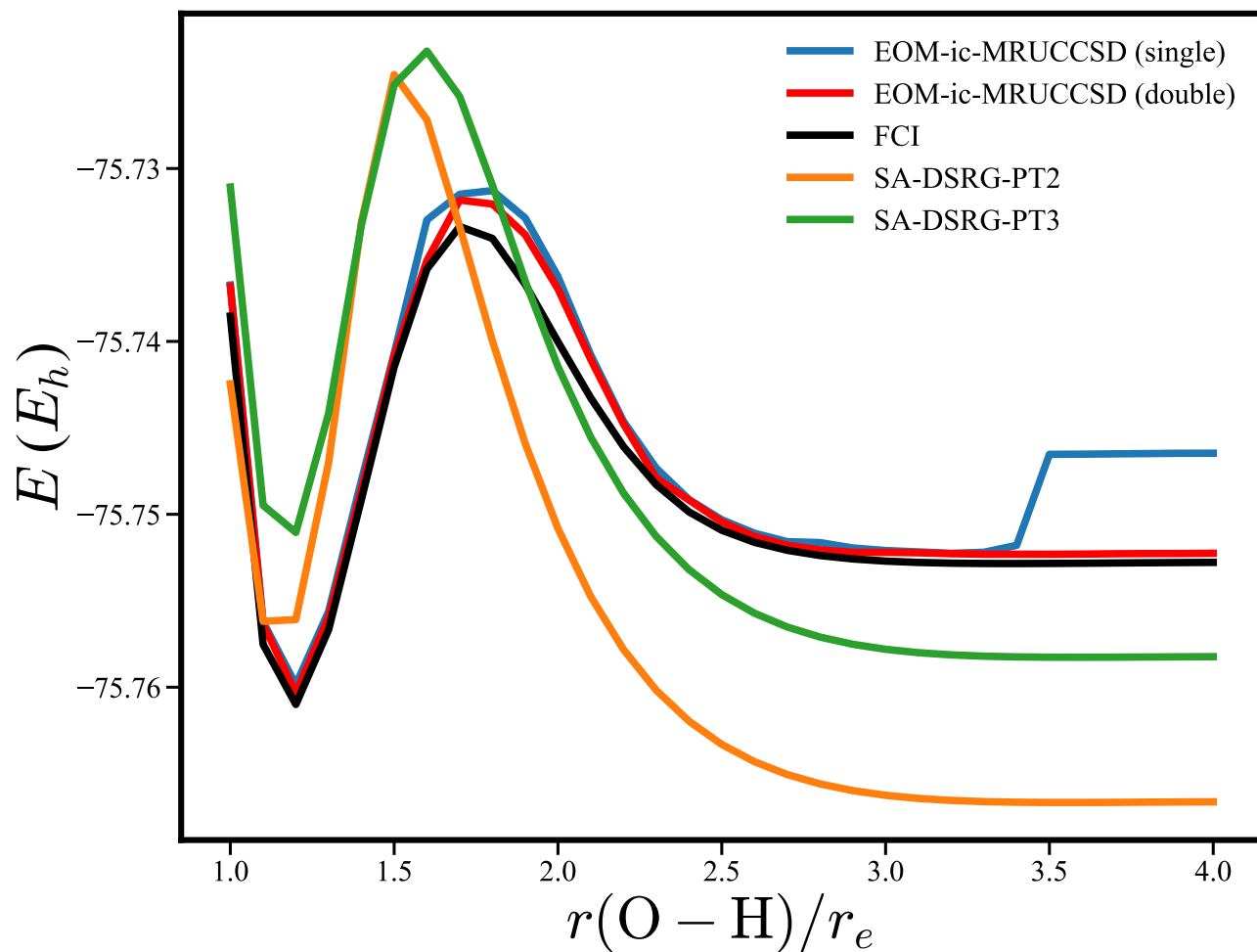


FIG. S2. Potential energy curves for the 1^1A_1 state of water the symmetric dissociation path computed with different multireference methods. This plot highlights the different behavior of the EOM-ic-MRUCCSD method when using one orthogonalization threshold (single) $\eta = 10^{-5}$ vs. two distinct orthogonalization thresholds (double) $\eta_1 = 10^{-5}$ and $\eta_2 = 10^{-8}$.

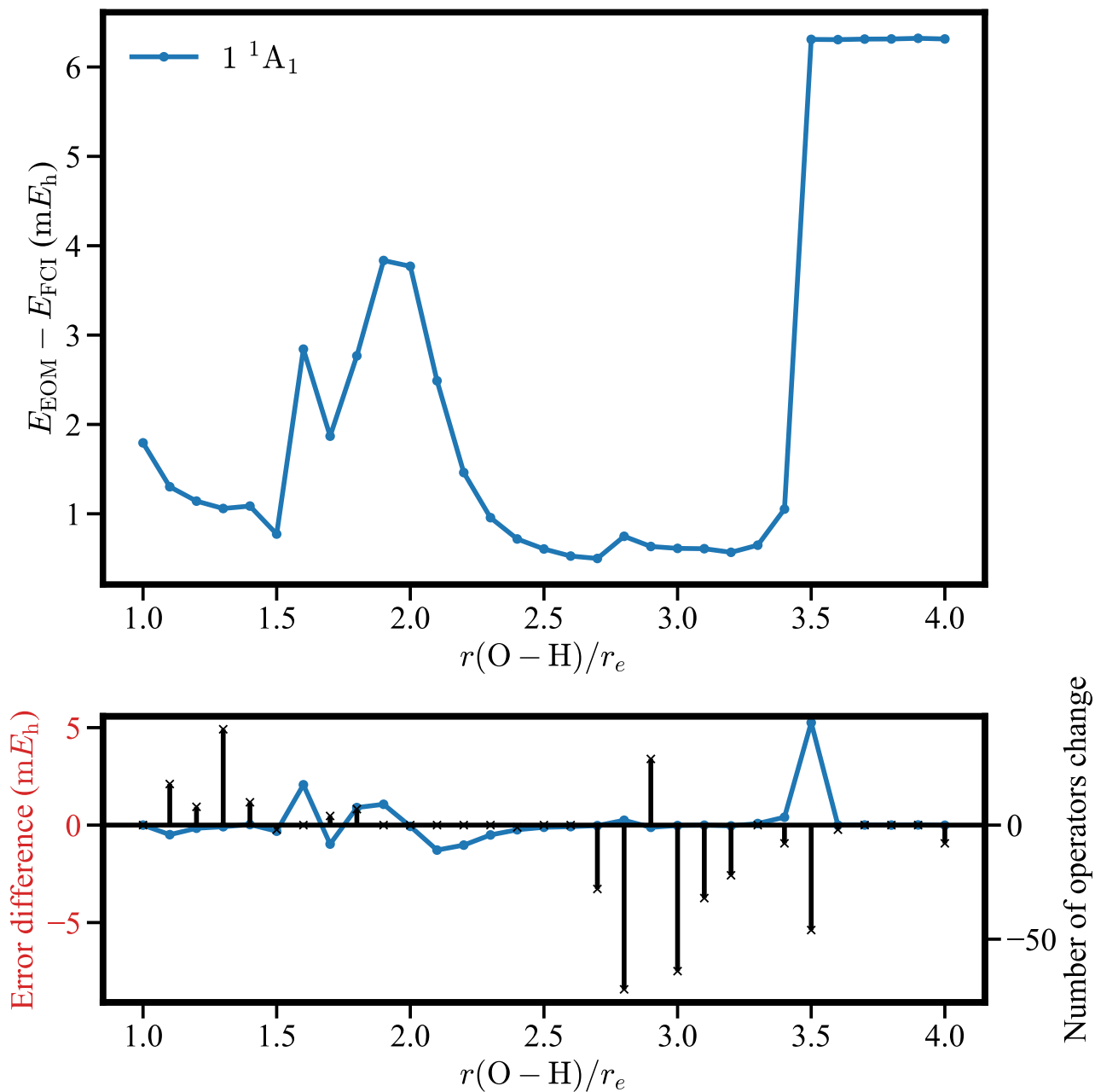


FIG. S3. The top panel: potential energy error curves (with respect to FCI) for the 1^1A_1 state of the symmetric dissociation of the water computed with the EOM-ic-MRUCCSD method and internal singles and doubles. Single threshold $\eta = 10^{-5}$ is used to eliminate linear dependencies. The lower panel: the change in the number of orthogonal operators and the energy errors with respect to the previous point (to the left).